

Carbonaceous aerosols over the Indian Ocean during the Indian Ocean Experiment (INDOEX): Chemical characterization, optical properties, and probable sources

O. L. Mayol-Bracero, R. Gabriel, and M. O. Andreae

Biogeochemistry Department, Max Planck Institute for Chemistry, Mainz, Germany

T. W. Kirchstetter and T. Novakov

Lawrence Berkeley National Laboratory, Berkeley, California, USA

J. Ogren and P. Sheridan

Climate Monitoring and Diagnostics Laboratory, NOAA, Boulder, Colorado, USA

D. G. Streets

Decision and Information Sciences Division, Argonne National Laboratory, Argonne, Illinois, USA

Received 9 October 2000; revised 4 May 2001; accepted 20 June 2001; published 11 October 2002.

[1] We measured carbonaceous material and water-soluble ionic species in the fine fraction ($D_p < 1.3 \mu\text{m}$) of aerosol samples collected on NCAR's C-130 aircraft during the intensive field phase (February–March 1999) of the Indian Ocean Experiment (INDOEX). Polluted layers were present over most of the study region north of the equator at altitudes up to 3.2 km. The estimated aerosol mass (sum of carbonaceous and soluble ionic aerosol components) of fine-mode particles in these layers was $15.3 \pm 7.9 \mu\text{g m}^{-3}$. The major components were particulate organic matter (POM, 35%), SO_4^{2-} (34%), black carbon (BC, 14%), and NH_4^+ (11%). The main difference between the composition of the marine boundary layer (MBL, 0 to ~ 1.2 km), and the overlying residual continental boundary layer (1.2 to ~ 3.2 km) was a higher abundance of SO_4^{2-} relative to POM in the MBL, probably due to a faster conversion of SO_2 into SO_4^{2-} in the MBL. Our results show that carbon is a major, and sometimes dominant, contributor to the aerosol mass and that its contribution increases with altitude. Low variability was observed in the optical properties of the aerosol in the two layers. Regression analysis of the absorption coefficient at 565 nm on BC mass ($\text{BC} < 4.0 \mu\text{g C m}^{-3}$) yielded a specific absorption cross section of $8.1 \pm 0.7 \text{ m}^2 \text{ g}^{-1}$ for the whole period. The unusually high fraction of BC and the good correlation between the absorption coefficient and BC suggest that BC was responsible for the strong light absorption observed for the polluted layers during INDOEX. High correlation between BC and total carbon (TC) ($r^2 = 0.86$) suggest that TC is predominantly of primary origin. Good correlations were also found between the scattering coefficient at 550 nm and the estimated aerosol mass for the fine fraction. These yielded a specific scattering cross section of $4.9 \pm 0.4 \text{ m}^2 \text{ g}^{-1}$. The observed BC/TC, BC/OC, $\text{SO}_4^{2-}/\text{BC}$, and K^+/BC ratios were fairly constant throughout the period. These ratios suggest that between 60 and 80% of the aerosol in the polluted layers during INDOEX originated from fossil fuel and between 20 and 40% from biofuel combustion. **INDEX TERMS:** 0305 Atmospheric Composition and Structure: Aerosols and particles (0345, 4801); 0322 Atmospheric Composition and Structure: Constituent sources and sinks; 0345 Atmospheric Composition and Structure: Pollution—urban and regional (0305); 0365 Atmospheric Composition and Structure: Troposphere—composition and chemistry; 4801 Oceanography: Biological and Chemical: Aerosols (0305); **KEYWORDS:** carbonaceous aerosols; INDOEX; chemical characterization; optical properties; sources; aerosols

Citation: Mayol-Bracero, O. L., R. Gabriel, M. O. Andreae, T. W. Kirchstetter, T. Novakov, J. Ogren, P. Sheridan, and D. G. Streets, Carbonaceous aerosols over the Indian Ocean during the Indian Ocean Experiment (INDOEX): Chemical characterization, optical properties, and probable sources, *J. Geophys. Res.*, 107(D19), 8030, doi:10.1029/2000JD000039, 2002.

1. Introduction

[2] The Indian Ocean Experiment (INDOEX) was conducted during the Northeast Monsoon (i.e., winter monsoon) when polluted air from the Indian subcontinent and Asia mixes with pristine air masses from the Southern Indian Ocean over the tropical Indian Ocean. This convergence provides a unique opportunity for studying aerosols and their climatic effects. The objectives of INDOEX were to investigate how pollutants emitted in India and Southeast Asia are transported through the atmosphere and how they affect the atmospheric composition and solar radiation fluxes over the ocean [Lelieveld *et al.*, 2001; Ramanathan *et al.*, 2001].

[3] Carbonaceous aerosols, composed mainly of organic (OC) and black carbon (BC) comprise a significant fraction of the submicron aerosol mass. Organic carbon, usually the most abundant component of the carbonaceous aerosol, may be directly introduced into the atmosphere in particulate form or may condense by gas-to-particle conversion of volatile anthropogenic and biogenic precursor compounds. Black carbon is produced exclusively by incomplete combustion of fossil and biomass fuels and, therefore, it is used as a tracer for combustion.

[4] Carbonaceous aerosols may play a significant role in radiative forcing, with both OC and BC affecting the extinction of solar radiation [Groblicki *et al.*, 1981; Shah *et al.*, 1984; Novakov *et al.*, 1997b; Hegg *et al.*, 1997; Penner *et al.*, 1998]. OC has been mainly associated with light scattering of the solar radiation and contributes to a negative climate forcing. BC, the principal light-absorbing aerosol species, produces a positive climate forcing [IPCC, 1996]. Since these aerosol species are usually emitted together, they are often internally mixed, which complicates the computation of their radiative properties and climatic effects [Jacobson, 2000].

[5] Despite the potential importance of carbonaceous aerosols in radiative and climate forcing [IPCC, 1996; NRC, 1996], relatively little information is available in terms of its worldwide concentrations, sources, mechanisms of formation, and radiative and nucleative properties. Three possible reasons for this are (1) difficulties in the characterization of the carbonaceous material due to its chemical and physical complexity [Eatough *et al.*, 1993; Rogge *et al.*, 1993; Zappoli *et al.*, 1999], (2) large uncertainties caused by sampling artifacts [Novakov *et al.*, 2000a], and (3) scarcity of airborne measurements, which are more relevant to quantifying aerosol climate forcing than ground-based measurements [Novakov *et al.*, 1997b]. Most previous airborne measurements have concentrated on sampling and analyzing inorganic aerosol components, such as sulfate (SO_4^{2-}), which has relatively well-known physical and chemical properties. However, in airborne measurements over the Northeast Atlantic, Hegg *et al.* [1993] demonstrated that sulfate can sometimes constitute only a modest fraction of the aerosol mass, and that the nonsulfate aerosol component may play an important role in determining both the light scattering and cloud condensation nucleus activity of aerosols. Ground-based measurements at Caribbean and Pacific sites have suggested that this nonsulfate component is composed of carbonaceous material [Novakov and Penner, 1993; Rivera-Carpio *et al.*, 1996]. In a more recent

study involving airborne measurements over the East Coast of the United States, carbon was found to account for, on average, 50% of the total aerosol mass, and an enhanced contribution of carbon species to aerosol mass aloft (altitudes between 2 and 3 km) was observed [Hegg *et al.*, 1997; Novakov *et al.*, 1997b]. Another study, which involved airborne measurements covering latitudes from 9°N to 46°N and altitudes up to 19 km, demonstrated that upper tropospheric aerosols often contained more organic material than sulfate [Murphy *et al.*, 1998]. These results highlight the need to improve our knowledge of the chemical and optical properties of carbonaceous aerosols, so that we may better understand their effects on radiative forcing.

[6] In this paper, we present the results on the chemical composition and optical properties of fine aerosols (aerodynamic particle diameter, $D_p < 1.3 \mu\text{m}$) collected aboard the National Center for Atmospheric Research (NCAR) Hercules C-130 aircraft during the INDOEX intensive field phase (IFP). Mass concentrations for aerosol total carbon (TC), BC, and OC are presented and discussed in the context of simultaneously collected aerosol light scattering and absorption data. Possible sources for the aerosol species in the polluted layers are also discussed based on their chemical and optical properties, on the use of chemical tracers for fossil fuel and biomass burning, and on the information available for emissions of these species.

2. Method

2.1. Sampling

[7] Aerosol sampling was conducted on the NCAR C-130 aircraft, based on Hulule Island (4.2°N, 73.5°E), Republic of the Maldives, during INDOEX IFP in February–March 1999 cf. C-130 overview paper by [Clarke *et al.*, 2002]. A total of 18 research flights (RFs) were performed over the Indian Ocean region covering a range in altitudes from 0 to 6.5 km. Here, we present results from 13 of these flights.

[8] Samples were collected through the community aerosol inlet (CAI) of the aircraft. The CAI, about 6.7-m total length, is mounted on the side of the aircraft and projects ahead of the aircraft nose. It supplied sample air to multiple instruments, which subsampled isokinetically via individual sampling tubes of different diameters. The 50% cut-size of the CAI is about 3 μm ; and for particles near 1 μm , its efficiency is about 90% in the moist boundary layer (better for dry aerosol aloft) (A. Clarke, personal communication, 2000). A detailed description is given by Blomquist *et al.* [2001]. Temporal resolution for the collection of our samples was about 10 to 30 min in the boundary and pollution layers, and up to two and three hours in the free troposphere. The relative humidity (RH) averaged $70 \pm 17\%$ in the MBL and $30 \pm 16\%$ in the rCBL legs.

[9] Aerosol samples were collected on two stacked-filter units (SFUs) mounted in parallel (Figure 1). The SFUs were connected to one CAI pick-off tube of 1.8-cm i.d. They each consisted of two polyethylene 47-mm diameter filter holders (NILU) connected in series. During operation, a Nuclepore prefilter (PC Membrane, Corning Costar, nominal pore size 8.0 μm) was placed in the first stage of each unit. This filter collected the coarse fraction which consisted of particles

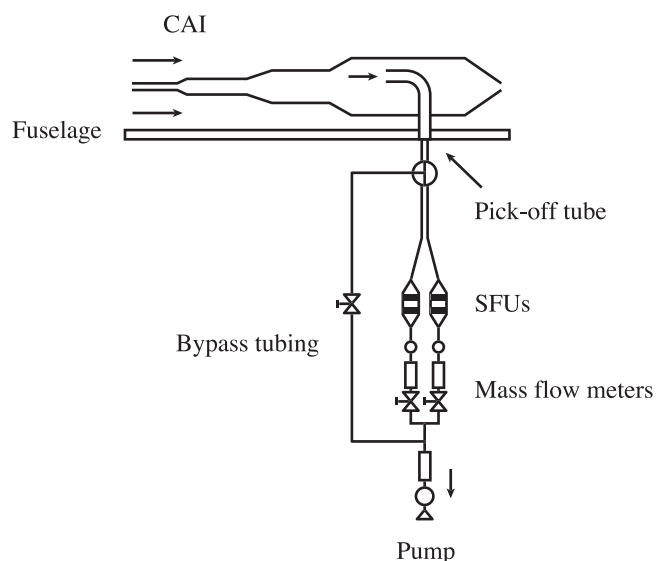


Figure 1. Filter sampler arrangement attached to the CAI of the C-130 aircraft. The bypass was used to maintain constant flow through the CAI when SFU samples were not being collected.

larger than ca. $1.3 \mu\text{m}$ (calculated for an average face velocity of 47 cm sec^{-1} in the boundary layer [John *et al.*, 1983]), and smaller than $3 \mu\text{m}$ (50% size-cut of the CAI) aerodynamic diameter.

[10] One SFU was used for the analysis of the carbonaceous component of the aerosols. In this unit, two quartz filters (Pallflex Tissuquartz 2500 QAT-UP) were placed directly on top of each other (tandem arrangement) in the second stage. The pressure drop across the tandem filter arrangement, for our face velocity of 47 cm sec^{-1} , was 25 inches of H_2O . This was calculated based upon the published change in pressure of $0.0013 \text{ atm per cm sec}^{-1}$ reported by McDow and Huntzicker [1990] for a tandem quartz filter arrangement. Before use, the quartz filters were baked at 800°C for 12 h to remove residual organic impurities. As discussed below (Section 3.1), the tandem arrangement was used to correct for the adsorption of gaseous organic compounds by the filter material, commonly referred to as the positive artifact [Kirchstetter *et al.*, 2001; Turpin *et al.*, 1994]. If not accounted for, this artifact results in an overestimation of organic aerosol mass concentrations.

[11] The second SFU was used for the analysis of water-soluble ions. The second stage of this unit had a PTFE Teflon membrane filter (Zefluor Membrane filter, Pall Gelman; nominal pore size $2.0 \mu\text{m}$, ($D_p < \sim 1.2 \mu\text{m}$)) to collect the fine aerosol fraction. Details of the analysis of this aerosol component are discussed by Gabriel *et al.* [2002].

[12] Loading and unloading of the filter units was performed before and after every flight in the laboratory facilities at Hulule Island. After the unloading process, filter samples were stored in a freezer at -18°C in precleaned glass vials until analysis. Vials were precleaned according to the procedures recommended by Salmon *et al.* [1998].

[13] Blank filters were collected on every flight using filter units loaded in the Hulule laboratory. These units were

connected to the aerosol inlet in the same manner as the real samples, with flow being applied for only 15 s.

2.2. Optical Measurements

[14] A three-wavelength nephelometer (Model 3563, TSI Incorporated, St. Paul, Minnesota USA), and a continuous light absorbing photometer (particle-soot absorption photometer, PSAP, Radiance Research Inc., Seattle, WA, USA) were operated at a RH of about 40% and used an impactor that allowed collection of particles of aerodynamic diameter less than $1 \mu\text{m}$ or $10 \mu\text{m}$. The nephelometer measured dry aerosol total scattering (σ_{sp}) and hemispheric backscattering of light at three visible wavelengths: 450, 550 and 700 nm . Here, we report σ_{sp} for particles of $D_p < 1 \mu\text{m}$ at 550 nm . At this wavelength, the detection limit for 30-second averages is 1 Mm^{-1} . The PSAP measured particle absorption (σ_{ap}) continuously via attenuation of 565-nm radiation by particles collected on a quartz filter. The PSAP data were adjusted to a wavelength of 550 nm using the correction scheme described by Bond *et al.* [1999]. PSAP results presented here also correspond to particles of $D_p < 1 \mu\text{m}$. The detection limit of this instrument is less than 1 Mm^{-1} for 1-min averages. Detection limits of both instruments decreased with longer averaging times; therefore, in our particular case (legs $\geq 10 \text{ min}$), these are conservative estimates. Sheridan *et al.* [2002] explain the operation of these instruments and discuss the uncertainties of σ_{sp} and σ_{ap} measurements.

2.3. Analysis

2.3.1. Carbonaceous Aerosols

[15] Quartz filter samples were analyzed for carbonaceous material at the Lawrence Berkeley National Laboratory (LBNL) with a thermal analysis method known as evolved gas analysis, EGA [Novakov *et al.*, 1997a, 1997b]. This method has been discussed in detail in several recent publications [e.g., Novakov *et al.*, 2000a]. Briefly, an aliquot of the sample (here, a punch of 4.4 cm^2 taken from the 13.2 cm^2 exposed area of the 47-mm quartz filters) is progressively heated at a linear rate (here, $20^\circ\text{C min}^{-1}$) in an oxygen atmosphere from 50°C to a suitable endpoint temperature, which is usually 650°C . The carbon-containing gases evolving from the sample are converted to CO_2 over a MnO_2 catalyst maintained at 800°C , and measured with a nondispersive infrared analyzer (Beckman Model 870). A plot of the mixing ratio of CO_2 as a function of temperature is called a thermogram, and the area under the thermogram curve is proportional to the TC content of the analyzed sample. Thermograms show a structure, often in the form of well-defined peaks, that is indicative of volatilization, decomposition, and combustion of the carbonaceous material (TC, BC, and OC) contained in the sample. The EGA method is quantitative for TC within $\sim 10\%$, shows a reproducibility of 3–5%, and has a detection limit of $\sim 0.2 \mu\text{g C}$ per sample [Dod *et al.*, 1979; Gundel *et al.*, 1984]. The difference between the pressure in the EGA instrument and the atmospheric pressure is less than 0.1%. Recently, to determine the precision of the EGA method, we analyzed several portions of a Hi-Vol sample that had been collected in a roadway tunnel. The coefficient of variation ($N = 7$) was 4, 6, 4, and 3% for TC, BC, OC, and the BC/OC ratio, respectively. Experiments involving many laboratories (carbon shootouts) have shown coefficients of

variation (CV) of about 9% for TC concentrations and between 30 and 50% for BC, depending the loading of the sample (lower CVs for lightly loaded samples) [Countess, 1990; Shah and Rau, 1990; Schmid *et al.*, 2001]. INDOEX C-130 samples were lightly loaded (much less than low-loaded samples presented by Schmid *et al.* [2001]), probably, with a CV in the range of 40 to 50% for BC.

2.3.2. Water-Soluble Ions

[16] The water-soluble species were determined at the Max Planck Institute for Chemistry (MPIC) using ion chromatography (for details, see Andreae *et al.* [2000] and Gabriel *et al.* [2002]). Water-soluble ions analyzed were Na^+ , NH_4^+ , K^+ , Mg^{2+} , Ca^{2+} , formate, methanesulfonate (MSA), Cl^- , NO_3^- , SO_4^{2-} , and oxalate. The detection limits in standard solutions are between 0.09 and 0.13 $\mu\text{mol L}^{-1}$ for cations, and 0.03 and 0.12 $\mu\text{mol L}^{-1}$ for anions. The uncertainty in the measurement is about 6%.

2.3.3. Air Mass Back Trajectories

[17] Air mass back trajectories (BTs) for up to ten days were calculated for every sampling leg using the hybrid single-particle Lagrangian integrated trajectories model, HYSPLIT-4 [Draxler and Hess, 1997] and the FNL meteorological data set produced by the U.S. National Center for Environmental Prediction. The vertical velocities from the FNL data set were used to derive the vertical transport component in the trajectory calculations. Trajectories were terminated at the aircraft location.

3. Results and Discussion

3.1. Interpretation of Thermograms

[18] Most of the INDOEX C-130 samples were collected from heavily polluted air masses. Their thermograms showed similar profiles, with carbon evolution extending to 600°C (Figure 2). Samples collected south of the Inter-tropical Convergence Zone (ITCZ) resulted in relatively featureless thermograms (not shown here), most likely due to the pristine conditions existing there.

[19] In general, thermograms of front filter samples collected in polluted air masses consist of several discrete peaks. For example, those of the front filters shown in Figure 2 consist of four peaks (i.e., A, B, C, and D). The first peak (A), representing the most volatile material in the sample, has a maximum intensity around 100°C and extends to ~200°C. Frequently, thermograms of backup filters (solid squares in Figure 2) show a peak at the same temperature and of similar intensity. The front filter removes all particles from the sampled air stream. Therefore, the origin of peak A on the backup filter is the adsorption of organic compounds that were originally present in the gas phase, and which adsorb to the front and backup filters during sampling [Kirchstetter *et al.*, 2000]. Sometimes, inhomogeneity in the filter stock could produce differences between the intensities of the volatile peak in front and back filters [Kirchstetter *et al.*, 2001]. In such cases, peak A is not included in the integration of the thermogram. The second peak (B) in Figure 2 is completely absent from the back filter, indicating that it is in the particulate phase. Similarly, peak C is more prominent in thermograms of front filters than back filters, indicating the collection of particulate-phase OC. Peak C in thermograms of backup filters may have been the result of adsorbed gases or low-level contamination.

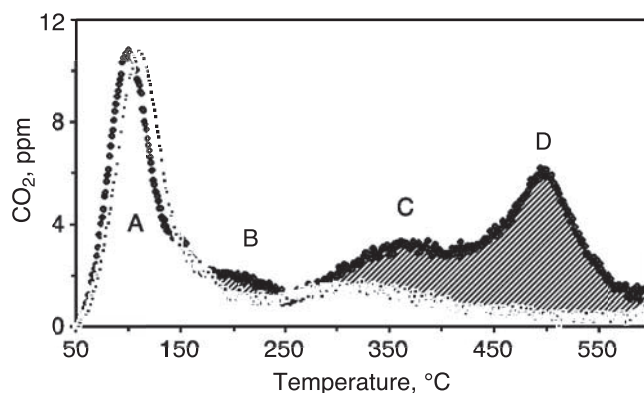


Figure 2. Example of a thermogram for front (open circles) and back (solid circles) quartz filters. The shaded areas are proportional to the TC aerosol concentrations. Assignments of peaks labeled A, B, C, and D are discussed in section 3.1. This sample corresponds to RF10 (9 March 1999), Northern Hemisphere (1.9°N, 74.6°E), altitude 83 m, $\sigma_{\text{sp}} = 92 \text{ Mm}^{-1}$, $\sigma_{\text{ap}} = 17 \text{ Mm}^{-1}$, $\omega_o = 0.84$.

[20] In environments influenced by combustion sources, such as the INDOEX region, the particle-phase carbonaceous material consists of both OC and BC. The high-temperature thermogram peak (D), which was centered at about 500°C and which is not present in thermograms of backup filter samples in the majority of cases, is used to estimate the amount of BC in the sample. To calculate the area under peak D (BC peak), we integrated the carbon evolving at temperatures above the minimum between peaks C and D, when these two peaks were well separated. In cases where these two peaks were not so well resolved, we looked at the shape of peak D and if it showed to be symmetric (bell-shaped), then we integrated the higher temperature half of the peak and multiplied this area by 2 to get the total area. For cases where peaks C and D were not resolved enough to apply one of these 2 approaches (about 7% of the total number of samples), BC was not determined. It has been shown that the carbonaceous material giving rise to this high-temperature peak is largely responsible for visible light absorption [Gundel *et al.*, 1984].

[21] Based on the information obtained from the thermograms, it is possible to estimate the concentrations of the carbonaceous components (i.e., TC, BC, and OC) in the samples. The mass of carbonaceous material on the backup filter is subtracted from the mass of carbonaceous material on the front filter to correct for the adsorption artifact (assuming that the contribution of gas-phase organics, peak A, is the same on both filters). This difference is defined as total carbon aerosol, TC, and reflects the mass of particle-phase carbonaceous material collected on the front filter. The OC is estimated as the difference between TC and BC.

[22] One uncertainty in the determination of BC and OC concentrations is the possibility that OC may char (undergo pyrolysis) during thermal analysis, and then coevolve with BC. Similarly, highly refractory organic material in the sample may be indistinguishable from BC. Both occurrences would lead to an overestimate of BC concentration. These factors led Gundel *et al.* [1984] to conclude that a combination of thermal, optical, and solvent extraction methods

must be used to accurately estimate BC. Optical (light-absorption) and solvent extraction (treatment to remove organic material from the sample before it is analyzed for BC) methods were employed for only a small number of INDOEX samples. These few results indicate that BC determination was not affected by coevolving organic material. Furthermore, a positive characteristic of the EGA method chosen for this study is the use of pure oxygen as the carrier gas. Compared to similar thermal techniques that expose the sample to inert gas (nitrogen or helium), the use of pure oxygen minimizes charring of organic material [Lavanchy *et al.*, 1999].

[23] Many of the samples analyzed in this study produced a thermogram peak that evolved beyond the temperature normally associated with BC. Carbonate carbon, which is usually not encountered in submicron samples, has an evolution temperature greater than that of BC. Powdered coral (calcium carbonate), for example, produces a single thermogram peak centered at 655°C. While the literature states that exposure to hydrochloric acid vapor will rid the sample of carbonate [Chow *et al.*, 1993], this treatment did not remove, or even reduce, the magnitude of the high-temperature peak in question. As a result, it is not certain what material gives rise to this peak. We believe, however, that because this peak was found in thermograms of backup filters and blanks as well as front filters it is indicative of contamination and was not collected during sampling. Thus, the thermogram area beyond the evolution of BC was not included in the estimate of carbonaceous aerosol concentration.

3.2. Estimation of Particulate Organic Matter

[24] The OC determined with thermal methods such as EGA is the carbon mass concentration in the particulate organic matter (POM). A POM/OC conversion factor is frequently used to estimate POM mass from the OC content. However, this conversion is at best approximate because the molecular-to-carbon mass ratio is not precisely known [Turpin and Lim, 2001]. As reported by Turpin and Lim, these values can range from 1.2 to as high as 2.6, depending on the aerosol composition. This uncertainty could lead to errors in the determination of POM and, therefore, the aerosol mass. The factor used for our INDOEX samples was 1.7, which corresponds to an empirical formula of ca. $\text{CHO}_{0.5}$, since the sampled air masses were strongly influenced by anthropogenic emissions from fossil fuel and biofuel combustion. This POM/OC factor assumes that the organic aerosol species, in cases like this, will be less oxidized than in air masses influenced by natural organic aerosols.

3.3. Pollution Layers and Air Mass Back Trajectories

[25] During most of the INDOEX IFP C-130 flights, two polluted layers were observed within the boundary layer (Figure 3). Vertical profiles of σ_{sp} and dew point temperature along with the concentrations of sodium in the coarse fraction (which can be a tracer for sea salt in the MBL) were used to define these layers. The first one was the well-mixed marine boundary layer (MBL) reaching up to ~ 1.2 km. The second one was a residual continental boundary layer, rCBL, between 1.3 and ~ 3.2 km. This rCBL was formed when continental air masses originating from the Indian subcon-

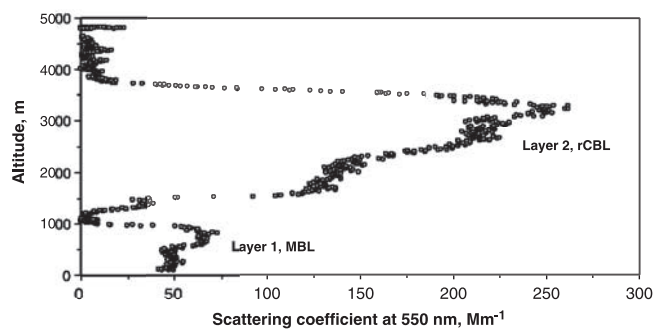


Figure 3. Vertical profile of σ_{sp} acquired over the Arabian Sea at around 0747 GMT on 16 March 1999 (RF 13). Layer 1 (MBL) is between 0 and ~ 1.2 km, and layer 2 (rCBL) between 1.3 and ~ 3.2 km.

continent were advected over the relatively cold ocean. The weaker convective activity over water could not sustain vertical mixing to the same height as over land. Therefore, a new MBL evolved at the base of the CBL, and the rCBL (between the top of the new MBL and the inversion at the top of the CBL) became disconnected from the free troposphere and the sea surface. More details about the mechanism of formation of the rCBL are presented by Johnson *et al.* [2000].

[26] Rasch *et al.* [2001] and Verver *et al.* [2002] present analyses of the meteorological conditions during the INDOEX IFP period. These analyses indicate that there was a significant change in the circulation patterns of the air masses between February and March. They divided the total period in two halves. The first half is what we call our “February period” (in which we include RFs 2 to 10). Here, air masses at surface levels in the Indian Ocean region were mainly coming in the northeast (NE) trades over the Western Bay of Bengal and/or in a flow from the NE, out of Southeast Asia (SEA). The second half is the “March period” (here, we include RFs 12, 13, 15, and 18) where air was coming mainly from a flow off the West Coast of India (the plume from Asia, SEA channel, was absent from March 1–22). These analyses were mostly limited to the near-surface level and/or below 2.5 km. This limits our knowledge in terms of the meteorological conditions prevailing for the rCBL. Also, RF 18 was not included in the analysis made by Rasch *et al.* [2001], since it was made on 25 March and their analyses ended on 22 March.

[27] Three major source regions were derived from the BT analyses: (1) India (INDIA), (2) Southeast Asia (SEA), and (3) West Asia (WA) (Table 1). Some samples were also collected in air masses that did not make contact with land over the past 10 days. They are classified as coming from the North Indian Ocean and/or the Arabian Sea (NIO), or coming from the South Indian Ocean (SIO). Flow from the northeast was evident in most of the trajectories, with most of the air masses originating from the Indian and south Asian subcontinents [Rasch *et al.*, 2001; Verver *et al.*, 2002]. The dominant source of aerosols in the Arabian Sea, the Bay of Bengal, and the NIO near the surface was India. At higher altitudes (above 1.2 km), contribution from other countries such as Asia, Arabia, and Africa was more evident, as suggested by the BTs and the analyses by Rasch *et al.* [2001].

Table 1. Summary of Results on the Chemical Characterization and Optical Properties of Aerosols collected on the C-130 Aircraft During INDOEX

Month	Flight	Sample	Altitude	Source	TC	BC	OC	OC'	POM	σ_{sp}	σ_{sp}	ω_0	EAM	% TC	% POM	% SO ₄ ²⁻	% BC	BC/TC	BC/OC	K/BC	SO ₄ ²⁻ /BC	SO ₄ ²⁻ /TC	BC/CO	CH ₃ CN/BC	
<i>Residual Continental Boundary Layer (rCBL)</i>																									
Feb	5	4	1.9	INDIA	4.7	—	—	—	—	20	82	0.81	—	—	—	—	—	—	—	—	—	1.23	—	—	—
Feb	5	6	2.8	INDIA	2.5	—	—	—	—	3.7	12	0.76	—	—	—	—	—	—	—	—	—	0.30	—	—	—
Feb	5	9	1.6	INDIA	12.2	5.5	6.7	6.6	11.1	27	115	0.81	29.8	41	37	29	19	0.45	0.83	0.08	1.57	0.71	0.020	—	
Feb	10	8	1.6	INDIA	13.0	4.7	8.3	8.1	13.8	33	151	0.82	26.3	49	53	18	18	0.36	0.57	0.09	0.98	0.35	0.014	—	
March	12	1	1.3	INDIA	3.4	1.3	2.1	2.1	3.5	13	55	0.81	—	—	—	—	—	0.38	0.61	—	—	—	0.006	—	
March	12	3	2.2	INDIA	5.8	1.4	4.4	4.4	7.5	15	67	0.81	—	—	—	—	—	0.24	0.31	—	—	—	0.006	—	
March	12	7	1.4	INDIA	5.2	1.1	4.1	4.1	6.9	15	64	0.81	—	—	—	—	—	0.22	0.28	—	—	—	0.006	—	
March	13	6	2.9	INDIA	15.7	6.3	9.4	9.3	15.8	38	197	0.84	41.3	38	38	31	15	0.40	0.67	0.15	2.00	0.80	0.018	0.05	
Feb	5	12	1.6	SEA	10.9	5.2	5.7	5.7	9.8	18	52	0.74	—	—	—	—	—	0.47	0.90	—	—	—	—	—	
March	15	9	3.2	SEA	3.4	1.6	1.8	1.8	3.0	12	49	0.81	9.1	38	33	23	18	0.47	0.89	0.19	1.30	0.61	—	—	
March	12	6	1.8	WA	5.9	2.3	3.6	3.6	6.1	23	102	0.82	—	—	—	—	—	0.40	0.66	—	—	0.010	—	—	
March	18	5	1.3	WA	5.9	2.6	3.3	3.1	5.3	20	78	0.79	14.4	41	37	28	18	0.44	0.80	0.15	1.52	0.68	—	0.06	
				Average	7.4	3.2	4.9	4.7	8.3	20	85	0.80	24.2	41	40	26	18	0.38	0.65	0.13	1.47	0.67	0.012	0.06	
				SD	4.4	2.0	2.6	2.5	4.3	10	50	0.03	12.8	5	8	5	1	0.09	0.22	0.05	0.38	0.31	0.006	0.01	
				N	12	10	10	10	10	12	12	12	5	5	5	5	5	10	10	10	5	5	7	2	
<i>Marine Boundary Layer (MBL)</i>																									
Feb	2	2	0.1	INDIA	8.0	4.0	4.0	3.9	6.7	20	74	0.79	19.7	40	34	32	20	0.50	1.01	0.10	1.60	0.80	—	0.02	
Feb	2	6	0.2	INDIA	4.4	2.4	2.0	1.9	3.3	16	76	0.83	16.9	26	19	46	14	0.54	1.19	0.22	3.23	1.76	—	0.03	
Feb	2	7	0.8	INDIA	6.0	2.9	3.1	3.0	5.2	22	85	0.79	20.0	30	26	40	14	0.48	0.92	0.19	2.77	1.33	—	0.03	
Feb	3	1	1.0	INDIA	7.2	3.2	4.0	3.9	6.7	20	65	0.76	16.2	44	41	30	19	0.44	0.79	0.09	1.52	0.67	—	—	
Feb	3	2	0.2	INDIA	8.2	3.1	5.1	5.1	8.6	27	92	0.77	20.1	41	43	31	15	0.38	0.61	0.11	2.03	0.77	—	—	
Feb	3	3	0.7	INDIA	—	2.4	—	—	—	20	66	0.77	—	—	—	—	—	—	—	0.20	2.60	—	0.04		
Feb	3	4	0.2	INDIA	4.9	2.4	2.5	2.4	4.1	21	81	0.79	16.1	30	26	42	15	0.49	0.95	0.21	2.89	1.41	—	—	
Feb	3	10	0.2	INDIA	5.8	3.2	2.6	2.6	4.4	22	99	0.82	19.0	30	23	43	17	0.55	1.22	0.18	2.55	1.40	—	0.03	
Feb	3	11	0.6	INDIA	5.1	2.8	2.3	2.3	3.9	26	86	0.77	19.2	27	20	46	14	0.54	1.18	0.18	3.19	1.73	—	—	
Feb	4	1	0.05	INDIA	8.7	2.6	6.1	6.0	10.2	8.0	66	0.89	17.7	49	58	20	15	0.30	0.43	0.06	1.32	0.40	0.010	—	
Feb	5	3	0.05	INDIA	13.3	5.7	7.6	7.5	12.8	27	90	0.77	27.8	48	46	24	21	0.43	0.76	0.08	1.19	0.51	0.021	—	
Feb	5	5	0.9	INDIA	6.2	2.8	3.4	3.4	5.7	21	65	0.76	17.2	36	33	33	16	0.45	0.82	0.16	2.07	0.93	—	—	
Feb	5	8	0.1	INDIA	—	3.1	—	—	—	28	98	0.78	—	—	—	—	—	—	—	0.12	2.25	—	—		
Feb	6	2	1.0	INDIA	—	2.4	—	—	—	20	85	0.81	—	—	—	—	—	—	—	—	2.61	—	—		
Feb	7	2	0.7	INDIA	3.1	1.7	1.4	1.4	2.4	11	40	0.78	9.0	34	27	43	19	0.54	1.18	0.07	2.33	1.26	0.007	—	
Feb	8	1	0.6	INDIA	9.6	4.0	5.6	5.6	9.5	20	74	0.79	—	—	—	—	—	0.42	0.71	0.08	—	—	0.016	—	
Feb	9	2	0.7	INDIA	3.9	1.9	2.0	2.0	3.4	13	52	0.80	—	—	—	—	—	0.48	0.91	—	1.50	0.72	—	—	
Feb	10	3	0.1	INDIA	3.3	1.6	1.7	1.7	2.8	15	60	0.80	9.1	36	31	37	18	0.49	0.97	0.11	2.07	1.02	0.008	0.06	
Feb	10	10	0.1	INDIA	6.2	1.8	4.4	4.3	7.3	20	97	0.83	16.8	37	43	30	11	0.29	0.41	0.11	2.83	0.83	0.008	—	
Feb	10	2 ^a	0.1	INDIA	2.7	1.5	1.2	1.2	2.0	18	67	0.79	7.9	35	26	39	19	0.55	1.25	0.12	2.04	1.13	0.008	0.07	
Feb	10	7 ^a	0.1	INDIA	4.7	2.3	2.4	2.4	4.1	26	122 ^a	—	13.9	34	29	40	16	0.48	0.94	0.11	2.45	1.19	0.009	—	
March	13	1	0.8	INDIA	—	1.0	—	—	—	12	48	0.80	—	—	—	—	—	—	—	0.31	—	—	0.005	—	
March	13	2	0.8	INDIA	2.7	0.9	1.8	1.8	3.0	7.0	28	0.80	9.7	28	31	43	10	0.34	0.52	0.26	4.52	1.56	0.006	—	
March	13	4	0.2	INDIA	8.1	2.3	5.8	5.7	9.8	15	43	0.74	19.3	42	51	25	12	0.29	0.40	0.16	2.11	0.60	0.012	—	
March	13	7	0.3	INDIA	<0.8	<0.4	<0.4	<0.4	<0.7	9.0	30	0.77	5.9	14	12	49	7	—	—	—	—	—	—	—	
March	15	2	0.8	INDIA	—	—	—	—	—	5.3	47	0.90	—	—	—	—	—	—	—	—	—	—	—	—	
March	15	3	1.1	INDIA	1.1	<0.4	0.9	0.9	1.5	5.3	51	0.91	—	—	—	—	—	—	—	—	—	—	—	—	
March	15	8	0.8	INDIA	1.7	<0.4	1.4	1.4	2.4	3.0	32	0.91	—	—	—	—	—	—	—	—	—	—	—	—	
March	18	4	0.9	INDIA	7.1	2.8	4.3	4.3	7.3	18	68	0.79	17.0	42	43	21	16	0.39	0.64	0.25	1.29	0.50	—	0.05	
March	18	6	0.9	INDIA	3.4	1.3	2.1	2.1	3.6	13	56	0.81	10.0	35	36	30	13	0.38	0.62	0.19	2.28	0.87	—	—	
Feb	3	5	0.7	NIO	4.3	1.6	2.7	2.6	4.5	12	36	0.76	11.0	39	41	32	14	0.37	0.60	0.18	2.21	0.83	—	0.05	
Feb	4	2	0.9	NIO	—	0.9	—	—	—	1.2	23	0.95	—	—	—	—	—	—	—	—	0.13	2.34	—	—	

Table 1. (continued)

Month	Flight	Sample	Altitude	Source	TC	BC	OC	OC'	POM	σ_{sp}	σ_{sp}	ω_0	EAM	% TC	% POM	% SO ₄ ²⁻	% BC	BC/TC	BC/OC	K ⁺ /BC	SO ₄ ²⁻ /BC	SO ₄ ²⁻ /TC	BC/CO	CH ₃ CN/BC	
Feb	4	3	0.04	NIO	—	—	—	—	—	1.2	11	0.90	—	—	—	—	—	—	—	—	—	—	—	—	
March	15	4 ^a	0.6	NIO	<0.4	<0.2	<0.2	<0.3	<0.3	3.6	46	0.93	4.5	9	7	58	4	—	—	—	—	—	—	—	
Feb	3	9	1.1	SEA	4.1	2.2	1.9	3.2	2.3	84	0.79	14.9	28	22	41	15	—	0.54	1.16	0.16	2.74	1.47	—	0.04	
March	18	3	0.1	SEA	4.3	1.7	2.6	2.5	4.3	15	0.79	13.1	33	33	31	13	—	0.40	0.67	0.34	2.33	0.94	—	0.08	
March	18	10	0.1	SEA	—	<0.4	—	—	—	5.8	21	0.78	—	—	—	—	—	—	—	—	—	—	—	—	
Feb	4	4	0.04	SIO	—	—	—	—	—	<1	1.6	—	—	—	—	—	—	—	—	—	—	—	—	—	
Feb	4	5	1.2	SIO	1.8	<0.4	1.6	1.6	2.7	<1	1.3	—	3.2	57	86	5	6	—	—	—	—	0.08	—	—	
Feb	9	3	0.1	WA	3.8	2.0	1.8	3.0	1.7	79	0.82	—	—	—	—	—	—	0.52	1.09	—	—	1.72	0.010	—	
March	12	4	0.8	WA	4.2	0.9	3.3	3.3	5.7	11	0.82	—	—	—	—	—	—	0.21	0.27	—	—	—	0.005	—	
March	12	5	0.9	WA	1.8	0.6	1.2	1.2	2.0	7.0	0.82	—	—	—	—	—	—	0.35	0.54	—	—	—	0.004	—	
March	13	3	0.8	WA	3.7	1.6	2.1	2.1	3.6	7.7	0.78	10.6	—	35	34	33	15	0.42	0.73	0.16	2.23	0.94	—	—	
March	13	5	0.6	WA	<0.6	<0.3	<0.3	<0.3	<0.3	12	39	0.76	6.7	9	5	59	5	—	—	—	—	—	—	—	
March	15	7	0.1	WA	3.1	<0.4	2.7	2.7	4.6	2.4	33	0.93	7.4	41	61	21	5	—	—	—	—	0.51	—	—	
Average					5.0	2.3	3.0	2.9	5.0	15	56	0.81	13.8	34	34	35	14	—	0.43	0.81	0.16	2.35	1.0	0.009	0.04
SD					2.6	1.0	1.6	1.6	2.7	8	26	0.05	5.8	11	17	12	5	—	0.09	0.28	0.07	0.70	0.4	0.004	0.02
N					33	34	33	33	33	43	44	42	29	29	29	29	29	29	29	29	29	30	28	19	12
Minimum					1.1	0.6	0.9	0.9	1.5	1.2	1.3	0.74	3.2	57	86	5	4	—	2.1	0.27	0.07	0.98	0.08	0.004	0.02
Maximum					15.7	6.3	9.4	9.3	15.8	38	197	0.95	41.3	9	7	59	21	55	1.25	0.34	0.34	4.52	1.76	0.021	0.08
Average					5.7	2.5	3.4	3.4	5.7	16	62	0.81	15.3	35	35	34	14	—	0.42	0.77	0.15	2.22	0.93	0.010	0.05
SD					3.3	1.4	2.0	2.0	3.4	8	34	0.05	7.9	10	16	11	5	—	0.09	0.27	0.07	0.73	0.43	0.005	0.02
N					45	44	43	43	43	55	56	54	34	34	34	34	34	34	39	39	34	35	26	14	

^a σ_{sp} /EAM outliers.

Dates of flights: 2 (18 Feb), 3 (20 Feb), 4 (24 Feb), 5 (25 Feb), 6 (27 Feb), 7 (28 Feb), 8 (4 March), 9 (7 March), 10 (9 March), 12 (13 March), 13 (16 March), 15 (19 March), and 18 (25 March). Results are reported at STP. Altitude is in km; TC, BC, and OC mass concentrations are in $\mu\text{g C m}^{-3}$; POM and EAM are in $\mu\text{g m}^{-3}$; OC' = OC - (oxalate + MSA + formate); concentrations of oxalate, MSA, and formate were in $\mu\text{g m}^{-3}$; POM = OC' \times 1.7. EAM = estimated aerosol mass, BC + POM + water-soluble ions averages excluding the LODs; $\text{Mm}^{-1} = \times 10^{-6} \text{ m}^{-1}$; % values are calculated using only measurements for which both values of EAM and the relevant chemical species are known. — = could not determine because of lack of IC, EGA, CO, CH₃CN, or absorption data, or because in the LOD of the measurement. SO₄²⁻ and K⁺ results from Gabriel et al. (unpublished manuscript, 2002). CO results from T. Campos (personal communication, 2000). CH₃CN results from Reiner et al. [2001]. INDIA = India, Sri Lanka, Pakistan, Afghanistan, Bangladesh, SEA = Thailand, Malaysia. WA = Saudi Arabia, Iran, Africa. SD = Standard deviation. N = number of measurements. Mass concentrations in the low MBL need to be corrected by about 10% losses of submicron particles in the CAI.

Table 2. Average Mass Concentrations and Percentages of Major Aerosol Components During INDOEX^a

Source	Size cut	TC	BC	OC	OC'	POM	EAM	%TC	%POM	%SO ₄ ²⁻	%BC	References
INDOEX total	<1.3	5.7 ± 3.3	2.5 ± 1.4	3.4 ± 2.0	3.4 ± 2.0	5.7 ± 3.4	15.3 ± 7.9	35 ± 16	35 ± 16	34 ± 11	14 ± 5	this study
INDOEX rCBL	<1.3	7.4 ± 4.4	3.2 ± 2.0	4.9 ± 2.6	4.9 ± 2.5	8.3 ± 4.3	24.2 ± 12.8	41 ± 5	40 ± 8	26 ± 5	18 ± 1	this study
INDOEX MBL	<1.3	5.0 ± 2.6	2.3 ± 1.0	3.0 ± 1.6	2.9 ± 1.6	5.0 ± 2.7	13.8 ± 5.8	34 ± 11	34 ± 17	35 ± 12	14 ± 5	this study
INDOEX Feb	<1.3	6.2 ± 3.2	2.8 ± 1.2	3.6 ± 2.0	3.6 ± 2.0	6.1 ± 3.4	16.7 ± 6.5	38 ± 18	36 ± 16	33 ± 10	16 ± 3	this study
INDOEX March	<1.3	4.8 ± 3.3	1.9 ± 1.3	3.2 ± 2.0	3.1 ± 2.0	5.2 ± 3.5	13.0 ± 9.5	31 ± 13	32 ± 16	35 ± 13	12 ± 5	this study
INDOEX Feb rCBL	<1.3	8.2 ± 4.4	4.2 ± 1.9	6.3 ± 2.6	6.2 ± 1.6	10.6 ± 2.6	28.0 ± 2.5	45 ± 6	45 ± 11	23 ± 8	18 ± 1	this study
INDOEX Feb MBL	<1.3	5.7 ± 2.6	2.6 ± 1.0	3.2 ± 1.7	3.1 ± 1.7	5.3 ± 2.9	15.6 ± 5.6	37 ± 18	35 ± 16	35 ± 10	16 ± 3	this study
INDOEX March rCBL	<1.3	6.6 ± 4.6	2.6 ± 1.9	4.0 ± 2.8	4.0 ± 2.7	6.8 ± 4.7	21.6 ± 17.3	39 ± 2	36 ± 3	27 ± 4	17 ± 1	this study
INDOEX March MBL	<1.3	3.7 ± 2.2	1.5 ± 0.7	2.6 ± 1.4	2.5 ± 1.2	4.3 ± 2.5	10.4 ± 4.8	29 ± 13	31 ± 19	37 ± 14	10 ± 5	this study
INDOEX INDIA, total	<1.3	6.2 ± 3.5	2.7 ± 1.4	3.8 ± 2.2	3.7 ± 2.2	6.3 ± 3.8	17.7 ± 7.9	36 ± 8	34 ± 11	34 ± 9	16 ± 3	this study
INDOEX SEA, total	<1.3	5.7 ± 3.5	2.7 ± 1.7	3.0 ± 1.8	3.0 ± 1.8	5.1 ± 3.2	12.4 ± 3.0	33 ± 5	29 ± 7	32 ± 9	15 ± 2	this study
INDOEX WA, total	<1.3	4.1 ± 1.5	1.7 ± 0.8	2.6 ± 0.9	2.5 ± 0.9	4.3 ± 1.5	9.8 ± 3.5	33 ± 15	34 ± 23	35 ± 17	11 ± 7	this study
ARACHNE (95–97)	<2.0	—	1.2 ± 0.5	—	—	—	15.9 ± 5.9	—	19	47	2.6	Andreae et al. [2002]
TARFOX	<~5	4.9 ± 2.7	—	—	—	—	14.8 ± 15.5	51 ± 34	—	40 ± 23	—	Hegg et al. [1997]
ACE-2	<1.0	1.3 ± 0.9	0.4 ± 0.3	0.8 ± 0.7	—	—	—	—	—	—	—	Novakov et al. [2000a]
SCAR-B	<4.0	—	—	—	—	—	—	69 ± 6	—	2 ± 1	7 ± 1	Ferek et al. [1998]

^aLiterature values are shown for comparison. TC, BC, OC, OC' mass concentrations are in $\mu\text{g C m}^{-3}$. POM and EAM mass concentrations are in $\mu\text{g m}^{-3}$ and were calculated using OC'. Size cut in μm . Values presented are averages \pm standard deviation. % values are calculated using only measurements for which both values of EAM and the relevant chemical species are known (see Table 1). ARACHNE (Aerosol Radiation and Chemistry Experiment) Negev Desert, Israel, ground-based. TARFOX (Tropospheric Aerosol Radiative Forcing Observational Experiment) mid Atlantic coast, US, aircraft. SCAR-B (Smoke, Clouds, and Radiation-Brazil) Amazonia, Brazil, ground-based. — = data not available or not measured.

[28] Results reported in Table 1 are classified according to the tropospheric layers sampled (MBL or rCBL), the period that they represent (February or March), and the source region of the sampled air mass (INDIA, SEA, WA, NIO, SIO). Results from the samples collected in the free troposphere (>3.2 km) are not presented here. Table 2 provides a summary of the averaged values for the different classifications (i.e., layers, periods, and sources) and contains values from other studies for the purpose of comparison.

3.4. Mass Concentrations

[29] Significant variability between the mass concentrations of TC aerosol (from now on TC), BC, and OC was observed between samples from the same layers, periods, and/or source region, as it is shown in Table 1. However, the regionally averaged concentrations (INDIA, SEA, WA) for these species (Table 2 and Figures 4a and 4b) show low variability between them. Rasch et al. [2001] explain that the long residence times of aerosols (about 7 to 8 days for carbonaceous aerosols and sulfate) and the low wet deposition removal rate due to lack of rain during the winter/spring monsoon may be responsible for the great extent of polluted air masses over a large domain of the INDOEX region. These factors, assuming well-mixed layers, also could have resulted in the low regional variability in the average concentrations for the species under study. The following discussion pertains mainly to the samples collected in polluted air masses, below 3.2 km (in the MBL and/or rCBL), excluding the samples coming from oceanic regions (i.e., SIO and NIO) since these air masses were, in general, comparably unpolluted.

[30] Total aerosol mass in this study was calculated by summing the individual species measured (i.e., BC, POM (OC' \times 1.7), and the water-soluble ions) and does not include insoluble inorganic components (fly ash and mineral dust). OC' represents the OC after the subtraction of the carbon mass of the organic species determined by ion chromatography (i.e., oxalate, formate, and MSA). We refer to the total aerosol mass as “estimated aerosol mass” (EAM). The EAM ranged from 3.2 to 41.3 $\mu\text{g m}^{-3}$, with averages of 24.2 $\mu\text{g m}^{-3}$ and 13.8 $\mu\text{g m}^{-3}$ for the rCBL and the MBL, respectively. The average for the total period (MBL and rCBL) was 15.3 $\mu\text{g m}^{-3}$. These values are comparable to pollution levels observed in industrialized regions like the mid-Atlantic coast of the United States (TARFOX experiment), where the aerosol mass observed was on average about 15 $\mu\text{g m}^{-3}$ [Hegg et al., 1997], and in the Negev Desert in Israel (ARACHNE experiment) (highly influenced by anthropogenic sources) where this value was about 15.9 $\mu\text{g m}^{-3}$ [Andreae et al., 2002]. Figure 5 shows the contributions of aerosol species to EAM during the total INDOEX IFP. Major fractions were POM (35%), SO₄²⁻ (34%), BC (14%), and NH₄⁺ (11%). The contribution of the other water-soluble ions analyzed was about 6%.

[31] The uncertainty in the value of the POM/OC factor (see section 3.2) could have led us to an underestimation of the POM and, therefore, of the EAM for some of our samples. The magnitude of the error in these results is difficult to estimate due to the lack of knowledge about the appropriate POM/OC factors. However, if instead of 1.7, we apply 2.6, one of the highest values reported for POM/OC (for an aerosol heavily impacted by wood smoke) (Turpin

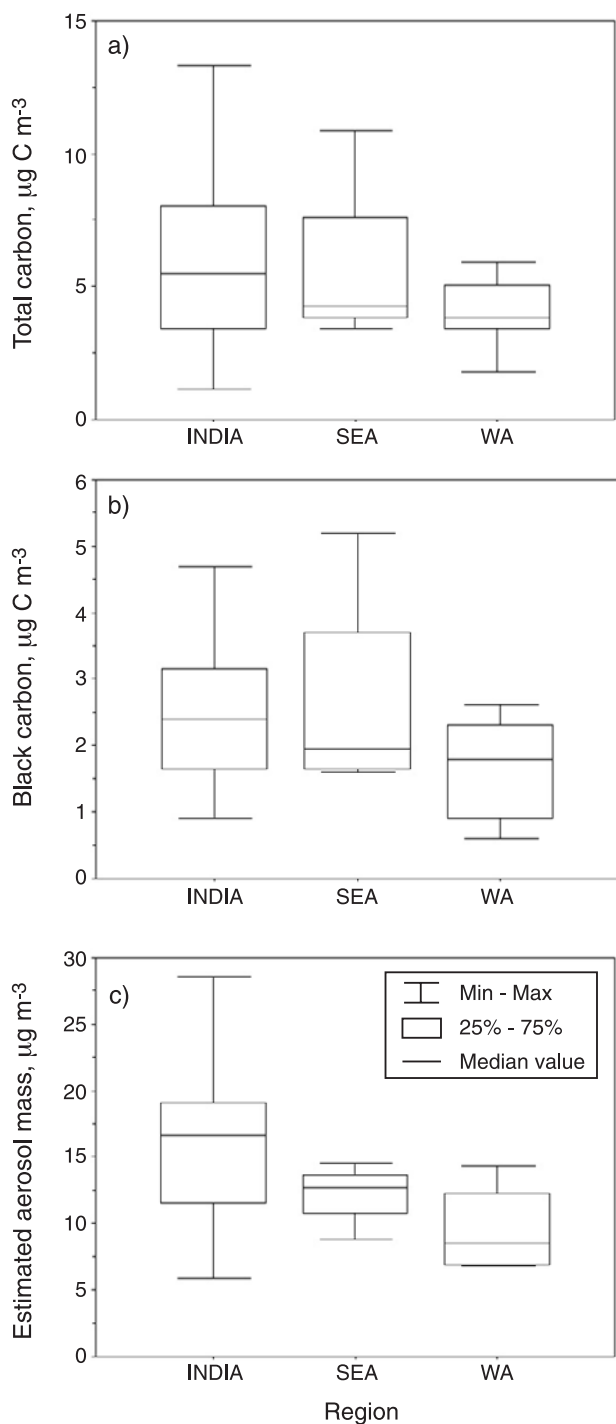


Figure 4. Mass concentrations of (a) TC, (b) BC, and (c) EAM as a function of air mass origin. Air mass regions are explained in section 3.3.

and Lim, submitted manuscript, 2000), to the mass concentrations of OC, the POM values would increase by a factor of 1.5. As a result, the EAMs would increase by about 10–16%, depending on their OC content. Since the INDOEX aerosol also has a contribution from fossil fuels, however, the POM/OC factor is unlikely to be greater than two, and consequently, EAM errors due to uncertainties about POM/OC are probably less than 10%.

[32] Concentrations of TC, BC, OC, and POM for the different periods and layers are presented in Tables 1 and 2. TC represents about 37% of the EAM. Table 2 shows that TC concentrations were much higher than in continental air masses during ACE-2 [Novakov *et al.*, 2000a], but comparable to the values obtained during TARFOX [Hegg *et al.*, 1997], suggesting very high levels of pollution. This was also supported by the high concentrations of BC (up to $6.3 \mu\text{g C m}^{-3}$) and OC (up to $9.4 \mu\text{g C m}^{-3}$) observed.

[33] The *t*-test was applied to the concentrations of TC, OC, BC, and EAM, and the differences between the February and March periods were found to be statistically significant only for BC ($p = 0.03$). It was found, however, that there were significant differences between the layers, especially during the February period, with the tendency for higher EAM and carbon fractions in the rCBL during the February period (Figure 6). The lowest EAM was found for particles measured in air masses coming from the WA region (Figure 4c). This is also supported by the results presented by G. Cautenet *et al.* (unpublished manuscript, 2002) whose model predicted the lowest concentrations of BC in the western part of the Indian Ocean. Removal processes, mainly dry deposition, as well as low amount of biofuel in comparison to SEA and INDIA could have been the reason for these lower aerosol burdens. For the SEA and INDIA regions, as well as for the layers within the March period, concentrations show low variability.

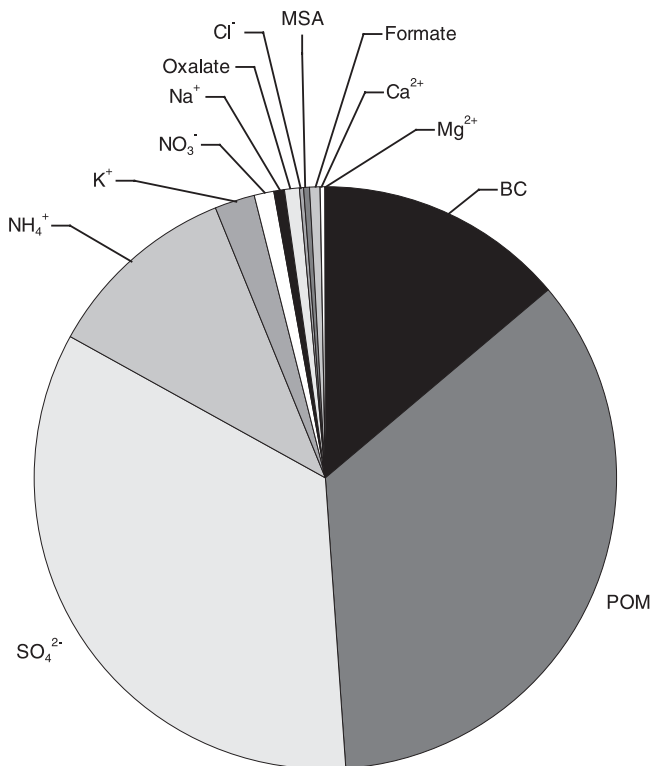


Figure 5. Polluted average aerosol composition for the fine fraction (altitude < 3.2 km). Estimated aerosol mass was $15.3 \pm 7.9 \mu\text{g m}^{-3}$. The major components were POM (35%), SO_4^{2-} (34%), BC (14%), and NH_4^+ (11%). The minor components were K^+ (2.1%), NO_3^- (1.0%), Na^+ (0.7%), oxalate (0.7%), Cl^- (0.5%), formate (0.3%), Ca^{2+} (0.3%), MSA (0.3%), and Mg^{2+} (0.1%).

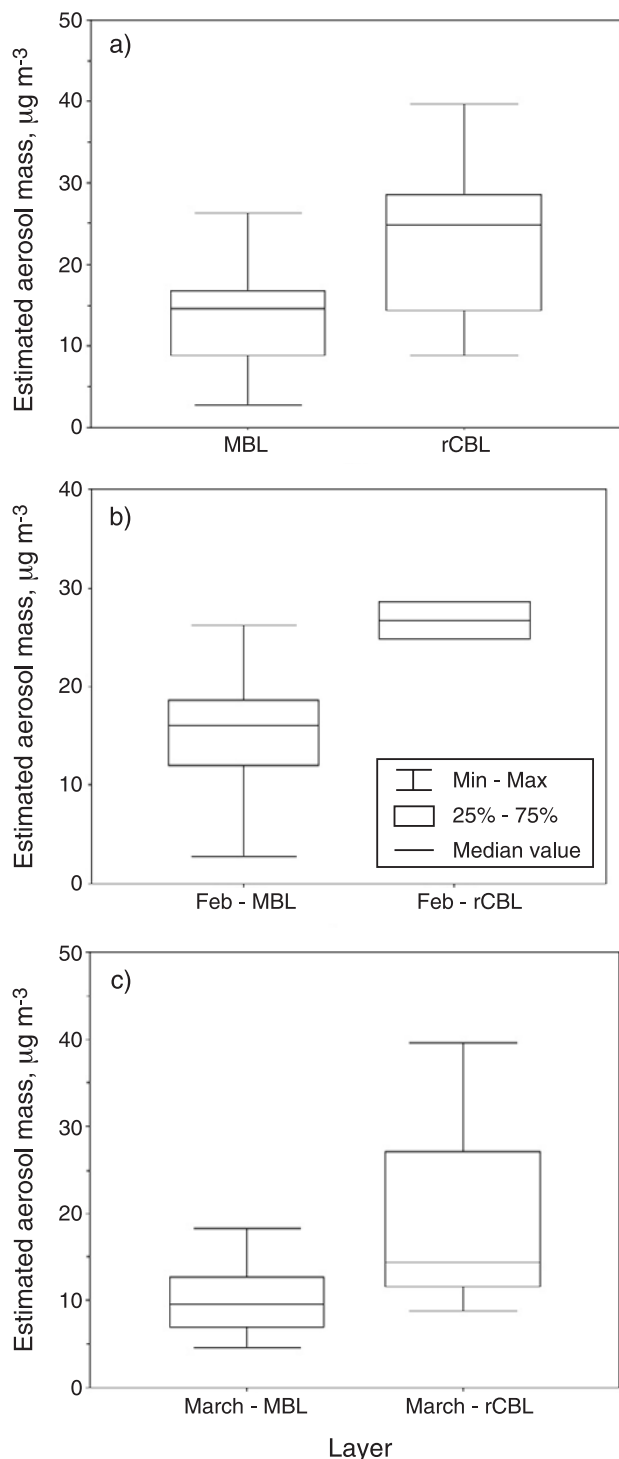


Figure 6. Aerosol mass concentrations as a function of layer (MBL and rCBL) and period (February and March); (a) total period, (b) February, and (c) March.

[34] It is also interesting to note that in the rCBL the %POM value (therefore, also %TC) was higher than the % SO_4^{2-} value (Table 2). Similar results were found for INDOEX-C-130 filter samples analyzed by scanning electron microscopy (M. Posfai, personal communication, 2000). Here, it was found that sulfate/soot particles were dominant in samples from RF 10 at 30 m (MBL), while at

1.5 km (rCBL), the majority of the particles were carbon spherules. During TARFOX (altitudes 0 to about 4.8 km), Novakov *et al.* [1997b] observed an increase in the carbonaceous fraction with increasing altitude. At even higher altitudes (upper troposphere) Murphy *et al.* [1998] also observed that aerosols contained more organic material than sulfate. In our case, this effect could have been due to a faster conversion of SO_2 into SO_4^{2-} in the MBL. This is supported by the results obtained on the R/V Ronald Brown (M. Norman, personal communication, 2000) where it was found that SO_2 represented only about 4% of the total sulfur (SO_4^{2-} plus SO_2) in the MBL, suggesting that most of the SO_2 had been converted into SO_4^{2-} . In contrast, a substantial fraction (up to about 65%) of the total sulfur was still present as SO_2 in the rCBL [Reiner *et al.*, 2001]. This finding highlights the importance of airborne studies, since ground-based measurements could significantly underestimate the contribution of carbon species to the column aerosol mass budget.

[35] Compared to the regions north of the ITCZ, the region south of the ITCZ was relatively unpolluted. Concentrations of TC, BC, and OC south of the ITCZ were often near or below the limit of detection (LOD, 0.2 to $0.8 \mu\text{g C m}^{-3}$) and, therefore, only a few results were obtained for this region (SIO in Table 1). The decrease in the carbon concentrations when approaching the Southern Hemisphere can be observed from the latitude profile of TC and BC over the Indian Ocean (Figure 7). High OC mass concentrations were concentrated in the Northern Hemisphere and were of the same magnitude as those of BC, in many cases, suggesting a primary origin for these aerosols. The influence of combustion-derived pollution is seen down to 5°S (north of the ITCZ). However, south of the ITCZ, where the BC reaches LOD values, the OC concentrations were low (i.e., $<3 \mu\text{g C m}^{-3}$). Therefore, we can infer that most of the OC north of the ITCZ has an anthropogenic origin.

3.5. Optical Properties of Carbonaceous Aerosols

[36] In this section, we compare our filter-based measurements with the scattering and absorption coefficients that were measured aboard the C-130 aircraft. To facilitate this comparison, the optical coefficients were averaged over the periods during which the filter samples were collected. A complete discussion of the entire optical-property data set is

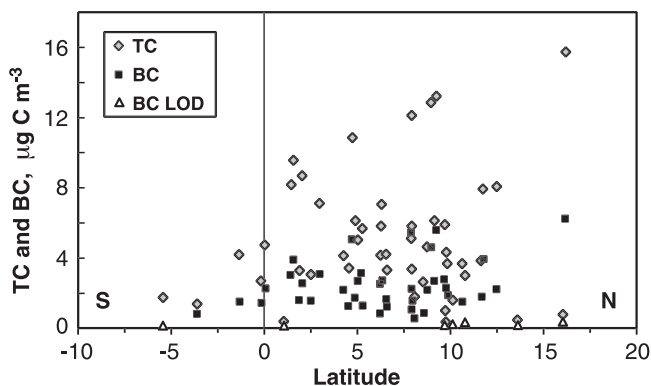


Figure 7. Latitude profile for TC aerosol and BC mass concentrations over the Indian Ocean.

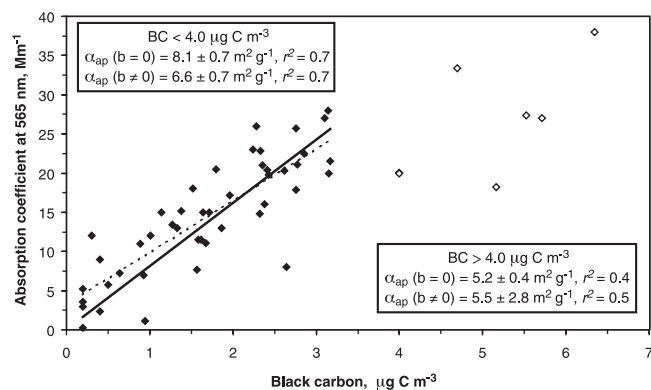


Figure 8. Regression analysis of aerosol light absorption coefficient as a function of BC mass concentrations. Solid diamonds represent $BC < 4.0 \mu\text{g C m}^{-3}$ and open diamonds represent $BC > 4.0 \mu\text{g C m}^{-3}$. The solid line was obtained when the intercept (b) was forced to zero, the dashed line is for $b \neq 0$.

presented by *Sheridan et al.* [2002]. We note here that the two data sets (chemical versus optical results) were obtained using different particle size cuts (1.3 versus $1.0 \mu\text{m}$) and sample relative humidities. However, preliminary analyses suggest that these differences introduce negligible error ($<1\%$) into the results discussed below (S. Howell, personal communication, 2000).

3.5.1. Specific Absorption Cross Section

[37] Black carbon is the main light-absorbing component of aerosol particles [*Rosen et al.*, 1978; *Gundel et al.*, 1984; *Lindberg et al.*, 1993]. An important optical parameter is the specific absorption cross section, α_{ap} ($\text{m}^2 \text{g}^{-1}$). Here we relate BC mass concentrations (in $\mu\text{g C m}^{-3}$) to the measured absorption coefficients, σ_{ap} (Mm^{-1}), to derive α_{ap} values for INDOEX aerosols. The data (Tables 1 and 3) show that σ_{ap} values for this subset of INDOEX samples ranged from 1.2 to 38Mm^{-1} , with an average for the polluted layers of 16Mm^{-1} . These values are considerably higher than those measured in other studies over polluted regions such as TARFOX and ARACHNE (i.e., 3 ± 3 and $9 \pm 4 \text{Mm}^{-1}$, respectively). The high INDOEX values demonstrate the highly light-absorbing nature of this aerosol. Figure 8 shows two distinctly different relationships of σ_{ap} versus BC concentrations below and above about $4 \mu\text{g C m}^{-3}$. As can be seen from this figure, the scatter in the data increased significantly for points with $BC > 4 \mu\text{g C m}^{-3}$. At present, we do not know the exact reason for these differences.

[38] The regression analysis of the first group of samples in Figure 8 ($BC < 4.0 \mu\text{g C m}^{-3}$), indicates a good correlation ($r^2 = 0.7$) and an α_{ap} value of $8.1 \pm 0.3 \text{m}^2 \text{g}^{-1}$ when the y-intercept is set to zero. This α_{ap} value is consistent with the typical range of α_{ap} values ($8\text{--}10 \text{m}^2 \text{g}^{-1}$) for BC originating from high-temperature combustion sources, and is in agreement with theoretical estimates [*Horvath*, 1993; *Liousse et al.*, 1993; *Malm et al.*, 1996]. An α_{ap} value of $6.6 \pm 0.6 \text{m}^2 \text{g}^{-1}$ was observed when the intercept was not forced to zero. At BC concentrations close to zero, absorbing species different from BC, and possibly not accounted for by our chemical analyses, could have been present. If a root-mean square analysis (RMS) is applied to this data set, the α_{ap} values

obtained are $8.1 \text{m}^2 \text{g}^{-1}$ and $8.3 \text{m}^2 \text{g}^{-1}$ for $BC < 4.0 \mu\text{g C m}^{-3}$ and $BC > 4.0 \mu\text{g C m}^{-3}$, respectively. These are the values presented in Table 3 and they show no significant differences between the absorption properties within the two layers. However, differences between the February and March periods are noticeable, with α_{ap} values of $10.8 \text{m}^2 \text{g}^{-1}$ and $5.6 \text{m}^2 \text{g}^{-1}$, respectively. These differences could have been, for example, due to differences in the mixing state or the absorbing properties of the BC.

[39] The observed α_{ap} values and the good correlation between the σ_{ap} values and BC mass concentrations for the whole period ($BC < 4 \mu\text{g C m}^{-3}$) suggest that BC is responsible for the strong light absorption observed in the dense brownish pollution haze over the Indian Ocean during INDOEX. This conclusion is further supported by the results of modeling studies [*Satheesh et al.*, 1999; *Podgorny et al.*, 2000].

3.5.2. Specific Scattering Cross Section

[40] The value of σ_{sp} is highly correlated with the mass of aerosol particles in the submicron diameter range [*Waggoner et al.*, 1981]. Therefore, the specific scattering cross section, α_{sp} , can be derived from the relationship between σ_{sp} and the total submicron mass. Values of α_{sp} reported in the literature are mostly determined by considering sulfate as the main scattering species. These values range from 1.8 to $13 \text{m}^2 \text{g}^{-1}$ [*Charlson et al.*, 1999; *Andreae et al.*, 2002]. However, sulfate is not the only important species when considering aerosol light scattering. Other chemical components can contribute significantly to the submicron mass of the atmospheric aerosol and, consequently, to the attenuation of visible wavelengths [*White*, 1990]. Fine carbonaceous aerosol is particularly important in this regard. During TARFOX, *Hegg et al.* [1997] demonstrated that carbonaceous aerosol can contribute, on average, about two thirds of the total dry aerosol scattering. Using their derived aerosol mass concentrations, they found a α_{sp} value of $2.8 \pm 0.3 \text{m}^2 \text{g}^{-1}$ ($r^2 = 0.77$).

[41] The two species that dominated the total aerosol mass in the INDOEX pollution layer were POM (35%) and sulfate (34%). In order to determine the relative contribution of these species to the σ_{sp} values, we attempted to use multiple linear regression analysis (MLR). However, statistical analyses showed that sulfate and POM are not statistically independent, probably sharing similar sources and sinks. As a result, it was not possible to derive separate α_{sp} values for these species from the MLR analysis. For this reason, we used the measured σ_{sp} values and the total estimated aerosol masses to determine the α_{sp} values (Figure 9).

[42] Dry σ_{sp} values for our samples ranged from 1.3 to 192Mm^{-1} (Table 1), with an average for the overall period of about 62Mm^{-1} . Similar results were obtained for the entire INDOEX-C-130 data set [*Sheridan et al.*, 2002]. The average and maximum values are comparable to σ_{sp} values obtained in regions influenced by anthropogenic emissions (Table 3) like the mid-Atlantic coast of the US during TARFOX (values ranged from $53\text{--}196 \text{Mm}^{-1}$), the Negev Desert in Israel during ARACHNE (average was 90Mm^{-1}), the continental air masses studied during ACE-2 (values ranged from 0.11 to 100Mm^{-1}), and a rural site in Hungary during the winter time (average of 93Mm^{-1}) [*Hegg et al.*, 1997; *Quinn et al.*, 2000; *Andreae et al.*, 2002]. In compar-

Table 3. Averages of Optical Aerosol Parameters (σ_{app} , σ_{sp} , ω_0 , α_{app} , and α_{sp}) During INDOEX Filter Measurements

Source	σ_{app} , Mm^{-1}	σ_{sp} , Mm^{-1} $\lambda = 550 \text{ nm}$	ω_0	α_{sp} , $\text{m}^2 \text{ g}^{-1}$		α_{sp} , $\text{m}^2 \text{ g}^{-1}$ (@ 550 nm)	References
				($\text{BC} < 4.0 \mu\text{g m}^{-3}$)	($\text{BC} > 4.0 \mu\text{g m}^{-3}$)		
INDOEX total	16 ± 8	62 ± 34	0.81 ± 0.05	8.1 ± 0.7 ($r^2 = 0.7$)	8.3 ± 2.4 ($r^2 = 0.4$)	4.9 ± 0.4 ($r^2 = 0.8$)	this study
INDOEX rCBL	20 ± 9	85 ± 50	0.80 ± 0.03	7.2 ± 1.8 ($r^2 = 0.6$)	nd	4.6 ± 0.7 ($r^2 = 0.9$)	this study
INDOEX MBL	15 ± 8	56 ± 26	0.81 ± 0.05	7.4 ± 0.8 ($r^2 = 0.6$)	nd	4.5 ± 0.5 ($r^2 = 0.7$)	this study
INDOEX Feb	18 ± 8	68 ± 33	0.80 ± 0.04	10.8 ± 1.6 ($r^2 = 0.5$)	7.7 ± 2.8 ($r^2 = 0.1$)	4.6 ± 0.7 ($r^2 = 0.5$)	this study
INDOEX March	12 ± 8	55 ± 36	0.82 ± 0.05	5.6 ± 0.8 ($r^2 = 0.7$)	nd	4.8 ± 0.4 ($r^2 = 0.9$)	this study
INDOEX Feb rCBL	20 ± 10	80 ± 49	0.79 ± 0.03	nd	nd	nd	this study
INDOEX Feb MBL	18 ± 7	65 ± 29	0.80 ± 0.05	10.8 ± 1.6 ($r^2 = 0.5$)	7.7 ± 2.8 ($r^2 = 0.1$)	3.7 ± 0.6 ($r^2 = 0.5$)	this study
INDOEX March rCBL	20 ± 10	91 ± 55	0.81 ± 0.01	7.2 ± 1.9 ($r^2 = 0.6$)	nd	4.5 ± 0.0 ($r^2 = 1$)	this study
INDOEX March MBL	9 ± 5	42 ± 12	0.83 ± 0.06	5.6 ± 1.2 ($r^2 = 0.6$)	nd	3.2 ± 0.9 ($r^2 = 0.3$)	this study
INDOEX INDIA	18 ± 8	72 ± 34	0.80 ± 0.04	8.0 ± 1.1 ($r^2 = 0.5$)	7.2 ± 0.9 ($r^2 = 0.6$)	4.9 ± 0.5 ($r^2 = 0.8$)	this study
INDOEX SEA	15 ± 6	53 ± 22	0.78 ± 0.02	nd	nd	nd	this study
INDOEX WA	13 ± 7	55 ± 27	0.82 ± 0.05	8.4 ± 1.5 ($r^2 = 0.8$)	nd	nd	this study
INDOEX NOAA/CMDL (0–1 km)	14 ± 7	58 ± 26	0.81 ± 0.05	–	–	–	Sheridan <i>et al.</i> [2002]
INDOEX NOAA/CMDL (1–3 km)	16 ± 10	74 ± 38	0.83 ± 0.06	–	–	–	Sheridan <i>et al.</i> [2002]
ARACHINE-96	9 ± 4	90 ± 30	0.92 ± 0.03	8.9 ± 1.3	–	3.0 ± 1.9	Formenti <i>et al.</i> [2001]
ARACHINE (95–97)	–	87 ± 54	–	–	–	5.2 ± 0.2	Andreae <i>et al.</i> [2002]
TARFOX	3 ± 3	44 ± 50	0.90 ± 0.09	–	–	2.8 ± 0.3	Hegg <i>et al.</i> [1997]
ACE-1	–	4.1 ± 2.8	0.99 ± 0.01	–	–	–	Quinn <i>et al.</i> [2000]
ACE-2, continental air	–	40 ± 17	0.95 ± 0.03	–	–	–	Quinn <i>et al.</i> [2000]
HUNGARY ^b	8.9	93	–	–	–	8.3 (for sulfate)	Mészáros <i>et al.</i> [1998]

^a Values of σ_{app} for TARFOX and Hungary were at 565 nm, INDOEX was 550 nm.

^b $D_p < 1 \mu\text{m}$, rural location, winter time. Literature values are shown for comparison.

α_{app} and α_{sp} for INDOEX were calculated using the RMS regression analysis. $1 \text{ Mm}^{-1} = 10^{-6} \text{ m}^{-1}$, NOAA/CMDL = National Oceanic and Atmospheric Administration, Climate Monitoring and Diagnostics. Values from NOAA/CMDL are for polluted air masses north of 5°N (STP). These averages correspond to the entire INDOEX optical-property data set. nd = could not determine because no data available or not enough data points for regression analysis. – = data not available or not measured.

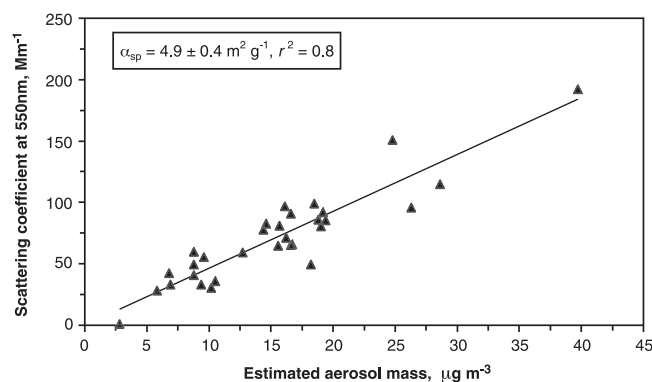


Figure 9. Regression analysis of aerosol light scattering coefficient as a function of estimated aerosol mass, EAM. The EAM is the sum of the mass concentrations of POM, BC, and water-soluble ions.

ison, values observed during ACE-1, where the anthropogenic influence was minimal (mainly natural maritime aerosols) were much lower (0.66 to 38 Mm^{-1}).

[43] Excluding three outliers (Table 1), for which α_{sp} would have physically impossible values, we found an α_{sp} value of $4.9 \text{ m}^2 \text{ g}^{-1}$ (using RMS analysis), with a very good correlation ($r^2 = 0.8$) (Figure 9). This value is close to values estimated by Penner *et al.* [1998] for ammonium sulfate ($5.07 \text{ m}^2 \text{ g}^{-1}$) and fossil fuel OC and BC ($4.84 \text{ m}^2 \text{ g}^{-1}$). Also, it compares well with the value of $5.2 \text{ m}^2 \text{ g}^{-1}$ obtained for the fine aerosol fraction during ARACHNE (1995–1997) [Andreae *et al.*, 2002].

[44] The values of α_{sp} presented in Table 3 show no significant differences within the different layers and sampling periods, suggesting aerosols of similar size distributions and/or refractive indices.

3.5.3. Single Scattering Albedo

[45] The single scattering albedo (ω_0), which is the ratio of scattering to total extinction, was estimated from the σ_{sp} and σ_{ap} values using the equation,

$$\omega_0 = \sigma_{\text{sp}} / (\sigma_{\text{sp}} + \sigma_{\text{ap}})$$

All values were between 0.74 and 0.95 (for dry conditions), with an average of 0.81 ± 0.05 for the polluted layers. Similar results for the entire INDOEX data set are presented by Sheridan *et al.* [2002] and are included in Table 3. A comparison with ω_0 values observed at other locations is also presented in Table 3. In general, INDOEX values of ω_0 were significantly lower than at other locations influenced by anthropogenic emissions (Table 2) and constant within the different periods and layers. This is consistent with the unusually high fraction of BC found (14% on average), suggesting that the chemical species responsible for this large absorption is indeed BC. Other studies have reported similar results in terms of the highly absorbing aerosol present over the Indian Ocean region [Ackerman *et al.*, 2000; Satheesh and Ramanathan, 2000].

[46] As outlined in the preceding two subsections and from Table 3, the optical properties of the INDOEX fine aerosol are not significantly different between the layers (MBL or rCBL). However, in the MBL, values of ω_0 and

α_{ap} (as mentioned before) along with the BC concentrations seem to vary between the two periods pointing to aerosols with a high absorbing character during the February period.

[47] The value of ω_0 determines the sign of the radiative forcing [Haywood and Boucher, 2000]. The low ω_0 values observed during INDOEX, resulting from the high fraction of BC (high absorption), result in a strongly negative radiative forcing of aerosols at the surface (-23 W m^{-2}), but a positive forcing at the top of the atmosphere ($+16 \text{ W m}^{-2}$) (Ramanathan *et al.*, unpublished manuscript, 2000). This could have significant impacts on climate. For example, a decrease in surface solar heating could decrease evaporation and thus the intensity of the hydrological cycle. Additionally, heating of the atmosphere could evaporate low-level trade cumulus clouds embedded within the aerosol layer resulting in a net warming influence [Ackerman *et al.*, 2000; Satheesh and Ramanathan, 2000; Ramanathan *et al.*, 2001].

3.6. Sources of Aerosols in the Polluted Layers

[48] During INDOEX IFP the dominant source region of aerosols in the study region (Arabian Sea, Bay of Bengal, and NIO) was India. In this country, for the year 1990, burning of biomass and fossil fuels contributed about 64% and 36% to the total fuel consumption, respectively. The largest contributions were from the burning of wood (33%), coal (30%), animal waste (14%), and agricultural residues (13%) [Venkataraman *et al.*, 1999].

[49] Most of the biomass burned in India is used as fuel for cooking and heating. Streets and Waldhoff [1998] estimated this value to be about 49% of the total energy consumption, mainly fuel wood (60%), crop residues (21%), and animal waste (19%). These values are similar to the ones presented by Venkataraman *et al.* [1999] for biomass (wood 51%, animal waste 22%, and agricultural residues 20%). The contribution of forest fires and burning of grassland is thought to be low (less than 7%).

[50] The major fossil fuels burnt in India are coal and diesel. Venkataraman *et al.* [1999] estimated a contribution of 49% from coal emitted in power plants, 8% from coal from the steel industry, and 8% from diesel. For 1996, Marland *et al.* [1999] calculated that coal and oil burning in India contributed 70% and 23%, respectively, to fossil fuel derived CO_2 emissions. Cooke *et al.* [1999] have also pointed out the dominant contribution of coal and diesel to fossil fuel burning. These estimates do not refer to recent years, however, so we have estimated emissions for the year 2000 using projections from the Regional Air Pollution Information and Simulation Model for Asia (RAINS-Asia 8.0) [Downing *et al.*, 1997]. These emissions reflect recent trends in fuel use and are determined from detailed energy-use data by fuel type and sector. Table 4 shows that direct coal combustion contributed 32% to total energy supply (22% from power generation and 10% from industrial manufacturing). Biofuels contributed 33%, and all oil products combined contributed 20%, the majority of which was diesel oil.

[51] The burning of fossil fuels and biofuels can release significant amounts of pollutants (gases and aerosols) into the atmosphere. The chemical analysis of the filter aerosol samples collected during INDOEX provided an opportunity to estimate the source strengths of these aerosols (e.g., fossil fuel or biomass burning), and to compare measurements

Table 4. Projections of Energy Use, BC, SO₂, and S Emissions in India for Year 2000

Fuel Type	Sector	Energy, PJ	BC Emissions, Gg yr ⁻¹	SO ₂ Emissions, Gg yr ⁻¹	S Emissions, Gg yr ⁻¹
Biofuel	residential	6740	399	229	114
Coal	power generation	4600	0.02	2740	1370
Coal	industrial manufacturing	2080	0.66	987.0	493
Heavy fuel oil	all	582	4.97	1030	516
Diesel oil	stationary sources	773	4.49	180	90
Diesel oil	transport	2020	53.1	470	235
Light fuel oil	all	856	1.47	142	71.1
Natural gas	all	1010	0	60.2	30.1
Other	all	2042	0	70.5	35.3
Process	industrial manufacturing	0	0	42.8	21.4
Total		20700	464	5950	2980

Gg = gigagrams = thousand metric tonnes. Process = non-combustion emissions from manufacturing processes. Source: year 2000 energy and SO₂ estimates from the RAINS-Asia Model 8.0. BC emission factors from *Streets et al.* [2001].

with predictions based on emissions factors. In the following sections, we will present (1) emissions that have previously been calculated for species that are tracers either for biomass or fossil fuel burning, (2) results for our chemical analyses for the species of interest, and (3) a comparison between emissions and field measurement results.

3.6.1. Emissions

3.6.1.1. Black Carbon

[52] As mentioned earlier, BC is a tracer for combustion. The Global Emissions Inventory Activity (GEIA) (<http://groundhog.sprl.umich.edu/geia>) provided the BC annual emission per square degree over the Indian region (G. Cautenet et al., unpublished manuscript, 2000). This inventory shows that carbonaceous aerosols from either biomass or fossil fuel combustion in India are mainly emitted from areas with a high population density and with a significant vegetated cover. Maxima are located in Bombay, Calcutta, and the Ganges region.

[53] *Streets et al.* [2001] have done extensive work on BC emissions for China. This work has involved a detailed reassessment of BC emission factors, paying particular attention to what fraction of emissions are truly in the BC size range (<1 μm or so in diameter) and what fraction of emissions are truly elemental carbon and not ash or organic carbon. This work has also assessed the performance of different kinds of combustors and the collection efficiency for BC of control devices such as electrostatic precipitators. We have applied the BC emission factors developed in this China work to the Indian situation. We have also used the RAINS-Asia model to estimate energy use, SO₂ emissions and BC emissions in India by fuel type and sector. Results are presented in Table 4, and represent projections for the year 2000 from the base year of 1995. Here, BC emissions

are estimated to be 464 Gg yr⁻¹ with a contribution of 86% from biofuel burning and 14% from fossil fuel combustion. Biofuel combustion in rural cookstoves and for heating in the north is the dominant contributor to BC emissions. The major fossil-fuel contributor to BC emissions is from diesel vehicles. Coal combustion for industrial steam raising and power generation does not, in general, lead to high BC emissions, because combustion conditions tend to burn out any BC that is formed.

[54] The work of *Streets et al.* [2001] enables us to estimate the ratios of BC to total particulate matter in emissions from the combustion of different fuels. This fraction is 0.75 for diesel vehicles, 0.23 for biofuels, 0.006 for industrial coal combustion, and 0.0003 for power-plant coal combustion.

[55] During INDOEX, *Dickerson et al.* [2002] estimated BC emission from the rate of CO emission in India and the ratio of BC to CO observed downwind. This analysis yielded 2–3 Tg (BC) yr⁻¹. To our knowledge, prior to INDOEX (this study and *Dickerson et al.* [2002]) the only detailed studies on emissions (segregated by sources) for carbonaceous aerosols in India have been carried out by *Reddy and Venkataraman* [2002a, 2002b]. In their first study, BC emission factors for fossil fuels (coal and petroleum) were from studies in Italy [*Bocola and Cirilo*, 1989] and the United States [*USEPA*, 1996]. These are not necessarily applicable to India. In a more recent study (BC data presented in Table 5), they derived the BC emission factors for coal using values for Indian specific technologies and air pollution control. For petroleum, they used BC emission factors reported in the literature. In both studies, the values used for biomass burning were from studies performed in India. A summary of these values for fossil fuel, biofuel, and

Table 5. Comparison of BC and Sulfur from Fossil Fuel, Biofuel, and Mixed Emissions in This Study with the Study of *Reddy and Venkataraman* [2002a, 2002b]^a

Source	This Study			<i>Reddy and Venkataraman</i> [2002a, 2002b]		
	BC	S	S/BC	BC	S	S/BC
Fossil Fuel	64.7	2860	44.3	106	2015	19.0
Biofuel	399	114	0.3	207	150	0.73
Mixed	463	2980	6.4	313	2165	6.9

^aBC and S emissions are in Gg yr⁻¹. BC emissions in this study are estimates based on the methodology applied to China by *Streets et al.* [2001]. S emissions in this study are from RAINS-ASIA model for the year 2000 (extrapolations from the 1995 base year). BC emissions from *Reddy and Venkataraman* [2002a, 2002b] are assuming 50% of time air pollution equipment in operation to account for malfunctioning of air pollution equipment. S emissions from *Reddy and Venkataraman* [2002a, 2002b] are for year 1996–1997. All S emissions are derived from SO₂ emissions.

mixed emissions is presented in Table 5 along with results from our analysis for the purpose of comparison.

[56] Additionally, a BC emission factor of $0.59 \pm 0.37 \text{ g kg}^{-1}$, has been estimated for biofuel from different previous works (not specifically for India) [Andreae and Merlet, 2001]. Further on, these values are used for the purpose of comparison.

3.6.1.2. Sulfur

[57] The main sources of sulfur gases to the atmosphere are industrial activities and fossil fuel burning [Spiro *et al.*, 1992]. Only small quantities are emitted during biomass burning [Andreae *et al.*, 1988; Crutzen and Andreae, 1990; Spiro *et al.*, 1992]. Andreae and Merlet [2001] have estimated an SO_2 emission factor of $0.27 \pm 0.30 \text{ g kg}^{-1}$ for biofuel burning. Oxidation of sulfur gases produces aerosol SO_4^{2-} . Sulfur species (i.e., SO_2 and aerosol SO_4^{2-}) can be used as tracers of anthropogenic pollution.

[58] The Emission Database for Global Atmospheric Research (EDGAR) [Olivier *et al.*, 1996] allows the determination of the SO_2 emissions per square degree over the Indian region (Cautenet *et al.*, unpublished manuscript, 2000). It is observed that, as well as for BC, the SO_2 production in India is mainly located along the western coast (Bombay), in the southern tip, on the eastern coast (between Madras and Calcutta), and in the northern part.

[59] The emissions of sulfur in India are better known than those of BC. There have been several studies on this topic [Spiro *et al.*, 1992; Olivier *et al.*, 1994; Streets and Waldhoff, 1998; Venkataraman *et al.*, 1999] and most agree that between 77 and 93% of these emissions are caused by fossil fuel burning and industrial activities rather than biomass burning. This is confirmed by the results from the RAINS-Asia model for the year 2000. We estimate that total emissions of sulfur in 2000 are $2980 \text{ Gg (S) yr}^{-1}$, of which 1863 Gg (63\%) originate from direct coal combustion in power and industry, 912 Gg (31\%) are derived from oil combustion, and only 114 Gg (4\%) are derived from biofuel combustion. Reddy and Venkataraman [2002b] obtained similar estimates (Table 5). Their estimated sulfur emissions are $2165 \text{ Gg (S) yr}^{-1}$ for the year 1996/97, of which 93% is from fossil fuel and 7% from biofuel. The difference between 2980 Gg and 2165 Gg could be entirely explained by growth in energy use between 1996/97 and 2000.

[60] Our estimates do not include the combustion of agricultural residues in the field after harvest nor combustion of vegetation as part of land-clearing operations or wildfires. These are extremely difficult estimates to make without detailed knowledge of activities during the period of experimental measurements. Nevertheless, when they occur, these activities are large sources of BC (but not SO_2).

3.6.1.3. Potassium

[61] Potassium (K^+) is a useful marker for biomass burning [Andreae, 1983; Andreae *et al.*, 1998]. It is released in large amounts during the combustion process because it is a major electrolyte in the cytoplasm of plants. On the other hand, it is not emitted in significant quantities by combustion of fossil fuels. The emission factor estimated for biofuel is $0.05 \pm 0.01 \text{ g kg}^{-1}$ [Andreae and Merlet, 2001]. No specific emission data are available for the Indian Ocean region.

3.6.1.4. Acetonitrile

[62] Acetonitrile (CH_3CN) is another unique marker for biomass burning. It is emitted from fires during the smol-

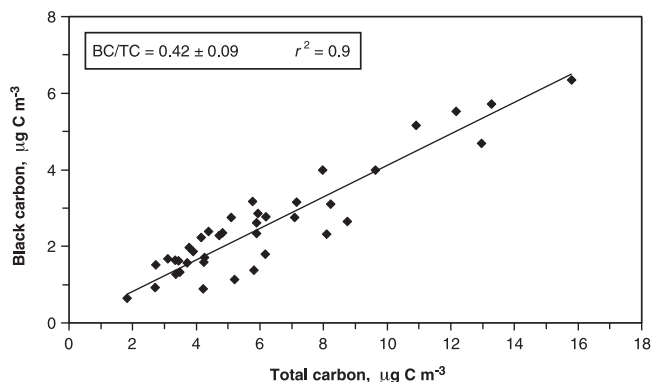


Figure 10. Regression analysis of BC versus TC aerosol.

dering phase [Lobert *et al.*, 1990] and it is not produced in large amounts in fossil fuel combustion. Its production from biomass burning is estimated to be between 0.4 and 1.0 Tg yr^{-1} , while the fossil fuel contribution (mainly from liquid fuels) is less than 0.03 Tg yr^{-1} [Holzinger *et al.*, 1999]. In biofuel, the estimated emission factor for this species is 0.18 g kg^{-1} [Andreae and Merlet, 2001]. No specific emission data are available for the Indian region.

3.6.1.5. Carbon Monoxide

[63] Carbon monoxide (CO) is another gaseous tracer for combustion, especially biomass burning [Crutzen and Andreae, 1990]. Its global production from biomass burning (748 Tg yr^{-1}) is much higher than its production from fossil fuel (300 Tg yr^{-1}) [Holloway *et al.*, 2000]. Lelieveld *et al.* [2001], using the EDGAR database [Olivier *et al.*, 1994], estimated that the CO anthropogenic emissions for the Indian region (including India, Bangladesh, Sri Lanka, Myanmar, Nepal, Pakistan, and Maldives) are 110 Tg yr^{-1} . It was also estimated that $\sim 70\%$ of the CO emitted in this region is from biofuel use and agricultural waste burning with approximately equal contributions from each [Lelieveld *et al.*, 2001]. A biofuel emission factor of $78 \pm 31 \text{ g kg}^{-1}$ for CO has been estimated [Andreae and Merlet, 2001].

3.6.2. Chemical Measurements

[64] In this section, ratios of the chemical tracers discussed above (i.e., BC, SO_4^{2-} , K^+ , CO, and CH_3CN) are used to provide information in terms of the emission sources of the aerosols in the INDOEX region. Table 6 presents (1) a summary of the average BC/TC, BC/OC, K^+/BC , $\text{SO}_4^{2-}/\text{BC}$, $\text{SO}_4^{2-}/\text{TC}$, BC/CO, and $\text{CH}_3\text{CN}/\text{BC}$ ratios during INDOEX, (2) these ratios calculated (when possible) for burning of biofuel (wood and agricultural residues) using emission factors from Andreae and Merlet [2001], and (3) the same information for previous studies in urban and industrialized regions (from the mid Atlantic coast of USA, Europe, Korea, and Japan), and in regions influenced by biomass burning (in Africa and Brazil).

3.6.2.1. Ratios of BC/TC and BC/OC

[65] The near constancy of BC/TC (0.42 ± 0.09) and BC/OC (0.77 ± 0.27) ratios for samples collected during the entire INDOEX period and the good correlation ($r^2 = 0.86$) between TC and BC (Figure 10) suggest that the INDOEX aerosol carbon is predominantly primary. If these species would have had similar source regions, the correlations could have been driven by meteorological factors. However,

Table 6. Indicators for Biomass Burning or Fossil Fuel During INDOEX^a

Source	BC/TC	BC/OC	SO ₄ ²⁻ /BC	S/BC ^b	SO ₄ ²⁻ /TC	K ⁺ /BC	BC/CO	CH ₃ CN/BC	References
INDOEX total	0.42 ± 0.09	0.77 ± 0.27	2.22 ± 0.73	0.74 ± 0.24	0.93 ± 0.43	0.15 ± 0.07	0.010 ± 0.005	0.05 ± 0.02	this study
INDOEX rCBL	0.38 ± 0.09	0.65 ± 0.22	1.47 ± 0.38	0.49 ± 0.13	0.67 ± 0.31	0.13 ± 0.05	0.012 ± 0.006	0.06 ± 0.01	this study
INDOEX MBL	0.43 ± 0.09	0.81 ± 0.28	2.35 ± 0.70	0.78 ± 0.23	1.00 ± 0.44	0.16 ± 0.07	0.009 ± 0.004	0.04 ± 0.02	this study
INDOEX Feb	0.46 ± 0.08	0.89 ± 0.20	2.24 ± 0.64	0.75 ± 0.21	0.98 ± 0.47	0.13 ± 0.05	0.012 ± 0.005	0.03 ± 0.01	this study
INDOEX March	0.36 ± 0.08	0.57 ± 0.19	2.18 ± 0.97	0.73 ± 0.32	0.80 ± 0.31	0.22 ± 0.07	0.008 ± 0.004	0.22 ± 0.19	this study
INDOEX Feb rCBL	0.38 ± 0.11	0.65 ± 0.27	1.27 ± 0.42	0.42 ± 0.14	0.65 ± 0.02	0.08 ± 0.01	0.017 ± 0.004	–	this study
INDOEX Feb MBL	0.47 ± 0.08	0.91 ± 0.25	2.32 ± 0.60	0.77 ± 0.20	1.05 ± 0.46	0.13 ± 0.05	0.011 ± 0.004	0.03 ± 0.01	this study
INDOEX March rCBL	0.39 ± 0.09	0.65 ± 0.21	1.61 ± 0.36	0.54 ± 0.12	0.70 ± 0.10	0.16 ± 0.02	0.009 ± 0.005	0.05 ± 0.01	this study
INDOEX March MBL	0.35 ± 0.07	0.55 ± 0.15	2.46 ± 1.08	0.82 ± 0.36	0.85 ± 0.37	0.24 ± 0.07	0.007 ± 0.003	0.19 ± 0.21	this study
Biofuel	0.11 ± 0.5	0.15 ± 0.6	0.70 ± 0.10	0.23 ± 0.40	0.081 ± 0.84	0.09 ± 0.3	0.008 ± 0.007	0.31 ± 0.16	Andreac and Merlet [2001]
Fossil fuel ^f	0.5 ± 0.05	1.0	–	–	–	0	–	0	–
ACE-2 (submicron), URB	0.38 ± 0.12	0.58 ± 0.22	15.2 ± 7.2	5.1 ± 2.4	5.5 ± 2.8	–	–	–	Novakov et al. [2000a]
Seoul, Korea, URB	0.43 ± 0.05	0.76 ± 0.1	–	–	–	–	–	–	Kim et al. [1999]
Sapporo, Japan, URB	0.49	0.97	1.1	0.37	0.55	0.04	–	–	Kaneyasu et al. [1995]
EXPRESSO Africa, BB	0.20 ± 0.06	0.22	0.44	0.15	0.08	0.085	–	–	Ruellan et al. [1999]
SCAR-B, Brazil, BB	0.10 ± 0.03	0.12 ± 0.03	0.28 ± 0.13	0.09 ± 0.04	0.03 ± 0.01	0.52 ± 0.11	–	–	Ferek et al. [1998]

^a Literature values are shown for comparison.
^b S/BC ratios are presented for comparison with ratios for emissions presented in the text. SO₄²⁻ and SO₂ values were converted into S (molecular interconversion).
^c Assumed from diesel, household coal dominated [Kleeman et al., 2000].

– = not available or not measured.

INDOEX values are arithmetic averages.

EXPRESSO (Experiment for Regional Sources and Sinks of Oxidants), Africa, savanna in the boundary layer, aircraft measurements.

URB = urban and industrial pollution.

BB = biomass burning.

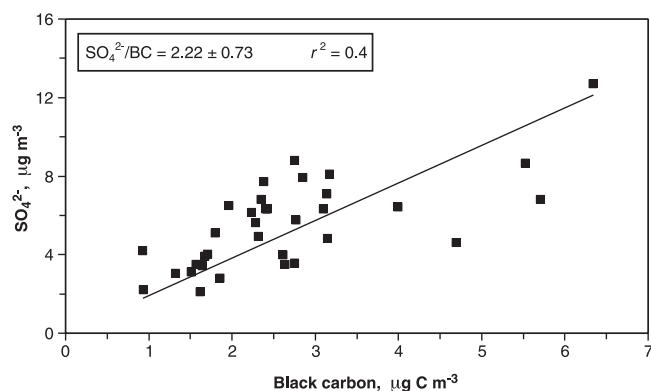


Figure 11. Regression analysis of SO_4^{2-} versus BC.

this does not seem the case because of the constancy of the ratios even when the BTs showed air masses of different origin (i.e., INDIA versus SEA versus WA). As shown in Table 6, the two ratios (BC/TC and BC/OC) are more similar to those measured in urban and industrial areas [Kaneyasu *et al.*, 1995; Kim *et al.*, 1999; Novakov *et al.*, 2000a] than in areas affected by biomass burning [Ferek *et al.*, 1998; Ruellan *et al.*, 1999].

3.6.2.2. Ratio of $\text{SO}_4^{2-}/\text{BC}$

[66] The aerosol SO_4^{2-} and BC measured during INDOEX are correlated, although r^2 is only 0.43 (Figure 11). The averaged $\text{SO}_4^{2-}/\text{BC}$ ratio was 2.22 ± 0.73 . This ratio is much lower in areas strongly influenced by biomass burning (Table 6), suggesting that much of the aerosol pollution in the Indian Ocean represents a mixture of biomass and fossil fuel combustion.

[67] It is important to note here that international shipping has been found to be a major source of sulfur emissions in Asia, with the route from the Persian Gulf to the Indian Ocean having one of the highest sulfur emissions (and possibly particulate matter too) due to the traffic of oil tankers [Streets *et al.*, 2000]. It is estimated that sulfur emissions in 1995 along this route were 53 Gg (S). This could be a possible reason for the higher $\text{SO}_4^{2-}/\text{BC}$ ratios observed at surface levels (cf. MBL samples with rCBL samples). This could also explain the results obtained on the R/V Ronald Brown during INDOEX, where an average $\text{SO}_4^{2-}/\text{BC}$ ratio of about 7.7 (about 3.5 times higher than our value) was found [Clarke *et al.*, 2002].

3.6.2.3. Ratios of K^+/BC

[68] The ratio of K^+/BC should be higher for biomass burning aerosol than for fossil fuel aerosol, since K^+ is emitted in high concentrations during most types of biomass burning [Andreae *et al.*, 1983, 1998] and BC is released in lower concentrations. However, the K^+/BC ratio is highly dependent on the type of biomass burned; therefore, its interpretation is not straightforward. A ratio of 0.15 ± 0.07 for K^+/BC was obtained during INDOEX. Comparison with emission factors and interpretation of these results are discussed in the following section (3.6.3).

3.6.2.4. Ratios of BC/CO and $\text{CH}_3\text{CN}/\text{BC}$

[69] BC/CO and $\text{CH}_3\text{CN}/\text{BC}$ ratios were calculated for our samples using the CO and CH_3CN mass concentrations obtained by Campos *et al.* (personal communication, 2000) and Reiner *et al.* [2001], respectively. This resulted in an

average ratio of 0.010 ± 0.005 for BC/CO and 0.05 ± 0.02 for $\text{CH}_3\text{CN}/\text{BC}$. There are no data available in the previous studies mentioned in Table 6 for the purpose of comparison. However, since CH_3CN background concentrations are in the range of 0.1 ppb or lower (D. Sprung, personal communication, 2000), the influence of biomass burning is evident from the fact that concentrations reached as high as 274 ppb in some of our samples.

3.6.3. Comparison of Measurements With Emissions

[70] Comparison of measured S/BC, K^+/BC , BC/CO and $\text{CH}_3\text{CN}/\text{BC}$, and BC/TC ratios with emission ratios is discussed in the following.

3.6.3.1. S/BC

[71] The sulfur species that was measured during the chemical analyses was aerosol SO_4^{2-} . However, to facilitate the comparison with the data on emissions, all SO_4^{2-} and SO_2 (either from measurements or emissions), and the ratios associated with them, were converted into S.

[72] The INDOEX S/BC ratio measured was 0.74 ($\text{SO}_4^{2-}/\text{BC} = 2.22$). The S/BC ratio calculated for mixed emissions (fossil fuel and biomass burning) in India is about 6.4 (Table 5). In the Indian region, it is estimated that approximately 51% (INDOEX period) of the SO_2 emitted is oxidized into SO_4^{2-} [Venkataraman *et al.*, 1999; Venkataraman, personal communication, 2000]. Assuming low variability in the concentrations of BC emitted and measured, this gives an estimated aerosol S/BC ratio of 3.3. The difference between the measured and the emissions ratios could be due to several factors.

[73] BC measurements can be readily compared with emissions because this species does not undergo chemical conversion when released into the atmosphere and is only subject to physical deposition processes. However, the case for sulfur species is different. First, not all the SO_2 emitted will undergo chemical conversion into aerosol SO_4^{2-} . Globally, only about 50% will undergo such transformation, principally by in cloud-oxidation which produces about 85% of the aerosol SO_4^{2-} , while the remaining 50% of SO_2 is removed by deposition processes [Chin *et al.*, 1996]. Despite the fact that it has been estimated that in India 51% of SO_2 will be oxidized to SO_4^{2-} , it is possible that due to the particular conditions during the INDOEX IFP, i.e., sparse cloud cover [Ackerman *et al.*, 2000], a smaller fraction of the SO_2 could have undergone such conversion. Also, the fact that SO_4^{2-} can be removed faster than BC by wet deposition could have resulted in lower S/BC ratios.

[74] Another possible explanation for the differences in these ratios is that the BC emissions may be underestimated. The BC emission factors that we are using to calculate S/BC were estimated based upon a methodology previously applied to China. Here, it is assumed that all industrial coal combustion in India has some level of particulate matter control. However, if there is significant uncontrolled coal combustion in the industrial sector, then the BC estimate would need to be increased. The role of local sources of emissions, such as emissions from the burning of fuel oil by international shipping, needs to be further investigated. Additionally, possible SO_4^{2-} underestimation or BC overestimation in the chemical analyses could have also contributed to these differences.

[75] If we now compare our S/BC ratio of 0.74 with the S/BC ratios calculated in this study for fossil fuel and

biofuel emissions (44.3 and 0.3, respectively), we find that our measurements seem to indicate a large contribution from biofuel emissions. This is also suggested by a comparison of the emissions from Reddy and Venkataraman [2002a, 2002b] with our ratio (Table 5). However, most of our results point to a major contribution from fossil fuel, with biofuel burning playing a lesser role. The reason for these differences is still not understood.

3.6.3.2. K^+/BC

[76] Since there are no data available on K^+ emissions in the Indian region, we use here the estimates presented by Andreae and Merlet [2001] for both K^+ and BC emissions from biofuel. Their data show a large difference between K^+/BC from the burning of wood fuel (~ 0.09) and non-wood biomass (~ 0.63). Assuming a K^+/BC ratio of 0.0 for fossil fuel and between 0.09 and 0.63 for biomass burning, a biomass burning contribution of 20% would yield a K^+/BC of 0.02–0.13. If the biomass burning contribution was 40%, the range would be 0.04–0.25. The K^+/BC ratio measured during INDOEX was 0.15 ± 0.07 . This suggests that the minimum biomass burning contribution, making the unlikely assumption that the biofuel mix contained no wood, would be 20%. However, the upper limit of this contribution is not possible to determine. In theory, it could have been up to 100% for a high wood fraction.

3.6.3.3. BC/CO and CH_3CN/BC

[77] For CO and CH_3CN , we followed the same approach as before. The estimated BC/CO ratio for biofuel is 0.007 ± 0.003 [Andreae and Merlet, 2001]. To estimate this ratio for fossil fuel, we used the CO global estimate for fossil fuel of 300 Tg yr^{-1} [Holloway et al., 2000] and the BC global estimate for fossil fuel of 5.1 Tg C yr^{-1} [Cooke et al., 1999]. This gives a BC/CO ratio of 0.017. Our INDOEX BC/CO ratio is 0.010 ± 0.005 . Therefore, although it is not clear which source dominated, it is evident that both contributed.

[78] In the case of the CH_3CN/BC ratio, the estimated value for biofuel was 0.31 ± 0.16 [Andreae and Merlet, 2001]. For fossil fuel, we assumed that this ratio is 0. The INDOEX ratio is 0.05 ± 0.02 , which suggests a strong contribution from fossil fuel emissions.

3.6.3.4. BC/TC

[79] We have left the discussion of BC/TC ratios until last because we want to use this ratio to address the question of what fraction of the aerosol observed during the INDOEX period was contributed by biomass burning (BB) and how much by fossil fuel (FF). This analysis is possible because the relative mass concentrations of BC and OC depend on the sources of the carbonaceous aerosol material and on the efficiency of the combustion process. During BB, the emissions of OC are much higher than the ones for BC, and the BC/TC ratio is typically 0.11 ± 0.03 , with relatively small variations between different types of burning (e.g., biofuel use and burning of agricultural waste [Andreae and Merlet, 2001]). However, during some types of FF combustion (e.g., diesel engines) the ratio of BC/TC is about 0.5, indicating that the concentrations of BC produced can be as high or higher than the concentrations of OC [Gillies and Gertler, 2000; Gillies et al., 2001; Kleeman et al., 2000; Lowenthal et al., 1994]. Consequently, BC/TC and BC/OC ratios in particles from BB can be significantly lower than in aerosol derived from FF combustion.

[80] In an attempt to estimate the contributions of FF and BB to the air masses under study, we (1) assumed a FF source with a BC/TC of 0.5 ± 0.05 , (2) used the estimated BC/TC ratio for BB of 0.11 ± 0.03 , and (3) used our INDOEX total averaged BC/TC ratio of 0.42 ± 0.09 . Contributions of BB and FF of about 20% and 80%, respectively, were obtained. Applying this reasoning to the different periods and/or layers presented in Table 6, we found that the contributions of BB and FF ranged from 10 to 40% and 60 to 90%, respectively, throughout INDOEX. Extreme cases were, for example, sample 2 from RF 2 (February period). Here, the BC/TC ratio was 0.5, which gives a 100% FF contribution. In the other extreme is sample 4 from RF 13 (March period) for which the BC/TC ratio was 0.29 and a 54% BB contribution was estimated. However, the predominant situation was when both biomass burning and fossil fuel inputs were contributing significantly. This is well illustrated with a sample collected in the rCBL during RF 13 (sample no. 6). Here, we found three indicators of BB in very high concentrations: (1) CH_3CN with a concentration of $0.31 \mu\text{g m}^{-3}$ (0.73 ppb) (D. Sprung, personal communication, 2000), (2) CO with a concentration of $343 \mu\text{g m}^{-3}$ (274 ppb) (T. Campos, personal communication, 2000), and (3) K^+ with a concentration of $0.98 \mu\text{g m}^{-3}$ [Gabriel et al., 2002]. These are the highest mass concentrations observed for CH_3CN , CO, and K^+ within our samples and they suggest the significant influence of biomass burning. However, the high concentration of SO_4^{2-} ($12.7 \mu\text{g m}^{-3}$), high ratios of BC/TC (0.40), BC/OC (0.67), and SO_4^{2-}/BC (2.0), and low ratio of K^+/BC (0.15) observed also indicate the significant influence of fossil fuel combustion. In this sample, we estimated a 74% FF contribution and a 26% BB contribution, which is close to the average values observed throughout the whole INDOEX period.

3.6.3.5. Comparison of Source Contributions for Different Periods and Layers

[81] In general, we observe that the contribution of fossil fuel dominates throughout the entire INDOEX period. The dominant emissions (fossil fuel or biomass) are, however, more evident when the data are segregated according to periods and layers (Table 6). The highest contribution of BB (still lower than the FF one) was observed in the rCBL and in the March period (lowest BC/TC, SO_4^{2-}/BC , and BC/CO ratios, and highest K^+/BC and CH_3CN/BC ratios). The K^+/BC and SO_4^{2-}/BC ratios were always higher in the MBL, probably due to the higher fraction of POM observed in the rCBL. Novakov et al. [2000b], in their preliminary analysis of the carbon, SO_4^{2-} , and K^+ content of samples collected on INDOEX C-130 RFs 2, 3, and 10 (flights belonging to our February period), concluded that FF combustion, and not BB, was the major source of the fine carbonaceous aerosols during INDOEX. This is true, especially for the February period and the MBL, as it is seen in Table 6. However, it is important to note the increase in the contribution of BB during the March period (as high as 40%). This increase in BB was probably due to the change in the meteorological conditions during the second half of the INDOEX period (as discussed by Rasch et al. [2001] and Verver et al. [2002] and as explained in section 3.2).

[82] Due to the major influence of fossil fuel and the high fraction of BC (and, therefore, strong absorbing character of

the polluted layer), we believe the predominant source of the INDOEX carbonaceous aerosols is diesel vehicles, poorly adjusted two-cycle engines, and open coal burning mostly generated in the Indian and South Asian subcontinents. The origin of the observed biomass burning seems to be biofuel, which is widely used in India, mainly for household purposes [Olivier *et al.*, 1994; Reddy and Venkataraman, 2002b]. However, long range transport of biomass burning from forest fires in SEA could also have had an influence in some of the samples, as indicated by the BTs especially during the March period (e.g., RF 18).

[83] As we have commented, emissions and measurements are not in total harmony. We pointed to a major signature of fossil fuel combustion in the observations (chemical measurements), but emissions point to a dominant signature of biofuel combustion. Further work is needed to reconcile emissions, atmospheric transport and conversion, and observations. It is clear that industrial and power generation coal use is predominantly concentrated in the northern half of the country, while biofuel use dominates in the southern half; diesel oil is used in cities. The patterns of emissions of BC and SO₂ are quite well understood, but how they relate to observed concentrations depends on the movement of air masses and the meteorological conditions encountered in route. For example, if conditions are largely dry and cloud-free, then less sulfate will be measured at the receptor site for a given quantity of SO₂ emitted. The distance from source to measurement site will also have a bearing on conversion and deposition rates. The role of local sources and the elevation of emissions from different sources types are also important. All these factors will be considered in future work on source identification.

4. Conclusions

[84] Presented here are results for the chemical composition, optical properties, and possible sources of fine aerosols collected during airborne measurements over the Indian Ocean during the winter monsoon (February–March) of 1999. The mean estimated aerosol mass for the polluted layers (rCBL and MBL), excluding insoluble inorganic components, was $15.3 \pm 7.9 \mu\text{g m}^{-3}$. The major contributing species were POM (35%), SO₄²⁻ (34%), BC (14%), and NH₄⁺ (11%). In the rCBL, the fraction of POM was found higher than SO₄²⁻, probably due to faster conversion of SO₂ into SO₄²⁻ in the MBL. The carbonaceous fraction was found to be a major and sometimes dominant contributor to the aerosol mass aloft. The good correlation between BC and TC suggests a predominantly primary nature of the INDOEX carbon aerosol.

[85] BC was present in unusually high concentrations and correlated quite well with the light absorption coefficient. A strong correlation was also found between σ_{sp} and the estimated aerosol mass. The high fraction of BC, along with the low ω_0 values observed, suggest that this species is responsible for the strong light absorption properties observed for the polluted layers. A highly absorbing aerosol (low ω_0 values) could have serious implications for climate (e.g., decreasing the intensity of the hydrological cycle and reducing the cloudiness associated with trade cumulus clouds).

[86] The information derived from our measurements (high BC/TC, BC/OC, SO₄²⁻/BC, and BC/CO ratios, coupled

with low ratios of K⁺/BC, and CH₃CN/BC ratios) suggest that the high pollution levels observed during INDOEX were mainly the result of fossil fuel-derived aerosols (60 to 90%). Notwithstanding this fact, the contribution of biomass burning was evident for most of the samples (10 to 40%), increasing during the March period and in samples collected in the rCBL. Emissions estimates for the source region, however, point to a dominant signature of biofuel combustion. Further work is needed to reconcile emissions, atmospheric transport and conversion, and measurements.

[87] **Acknowledgments.** We thank the pilots and crew of the NCAR C-130 for their assistance during the INDOEX research flights; the NCAR/RAF personnel for their technical support during the entire experiment; Detlev Sprung, and Christof Jost for the SO₂ data; Teresa Campos for the CO data; and the government and people of the Republic of Maldives for their hospitality. Also, the staff of the MPIC mechanical workshop are gratefully acknowledged for help with the construction of the sampling system. This research was supported by the German Max Planck Society and the U.S. National Science Foundation. Work at LBNL was supported by the U.S. Department of Energy.

References

- Ackerman, A. S., O. B. Toon, D. E. Stevens, A. J. Heymsfield, V. Ramanathan, and E. J. Welton, Reduction of tropical cloudiness by soot, *Science*, **288**, 1042–1047, 2000.
- Andreae, M. O., Soot carbon and excess fine potassium: Long-range transport of combustion-derived aerosols, *Science*, **220**, 1148–1151, 1983.
- Andreae, M. O., and P. Merlet, Emission of trace gases and aerosols from biomass burning, *Global Biogeochem. Cycles*, **15**, 955–966, 2001.
- Andreae, M. O., E. V. Browell, M. Garstang, G. L. Gregory, R. C. Harris, G. F. Hill, D. J. Jacob, M. C. Pereira, G. W. Sachse, and A. W. Setzer, et al., Biomass-burning emissions and associated haze layers over Amazonia, *J. Geophys. Res.*, **93**, 1509–1527, 1988.
- Andreae, M. O., T. W. Andreae, H. Annegarn, J. Beer, H. Cachier, P. le Canut, W. Elbert, W. Maenhaut, I. Salma, F. G. Wienhold, and T. Zenker, Airborne studies of aerosol emissions from savanna fires in southern Africa: 2. Aerosol chemical composition, *J. Geophys. Res.*, **103**, 32,119–32,128, 1998.
- Andreae, M. O., W. Elbert, R. Gabriel, D. W. Johnson, S. Osborne, and R. Wood, Soluble ion chemistry of the atmospheric aerosol and SO₂ concentrations over the eastern North Atlantic during ACE-2, *Tellus, Ser. B*, **52**, 1066–1087, 2000.
- Andreae, T. W., M. O. Andreae, J. Cafmeyer, C. Ichoku, W. Maenhaut, and L. Orlovsky, Light scattering by dust and anthropogenic aerosol at a remote site in the Negev desert, Israel, *J. Geophys. Res.*, **107**(D2), 10.1029/2001JD900252, 2002.
- Blomquist, B. W., B. J. Huebert, S. G. Howell, M. R. Litchy, C. H. Twohy, A. Schanot, D. Baumgardner, B. Lafleur, R. Seebaugh, and M. L. Laucks, An evaluation of the Community Aerosol Inlet for the NCAR C-130 Research Aircraft, *J. Atmos. Ocean Technol.*, **18**, 1387–1397, 2001.
- Bocola, W., and M. C. Cirillo, Air pollutant emissions by combustion processes in Italy, *Atmos. Environ.*, **23**, 17–24, 1989.
- Bond, T. C., and T. L. Anderson, Calibration and intercomparison of filter-based measurements of visible light absorption by aerosols, *Aerosol Sci. Technol.*, **30**, 582–600, 1999.
- Charlson, R. J., T. L. Anderson, and H. Rodhe, Direct climate forcing by anthropogenic aerosols: Quantifying the link between atmospheric sulfate and radiation, *Contrib. Atmos. Phys.*, **72**, 79–94, 1999.
- Chin, M., D. J. Jacob, G. M. Gardner, M. S. Foreman-Fowler, and P. A. Spiro, A global three-dimensional model of tropospheric sulfate, *J. Geophys. Res.*, **101**, 18,667–18,690, 1996.
- Chow, J. C., J. G. Watson, L. C. Pritchett, W. R. Pierson, C. A. Frazier, and R. G. Purcell, The DRI thermal/optical reflectance carbon analysis system: Description, evaluation and applications in U. S. air quality studies., *Atmos. Environ., Part A*, **27**, 1185–1201, 1993.
- Clarke, A., P. K. Quinn, and J. Ogren, The INDOEX aerosol: A comparison and summary of chemical, microphysical, and optical properties observed from land, ship, and aircraft, *J. Geophys. Res.*, **107**, 10.1029/2001JD000572, in press, 2002.
- Cooke, W. F., C. Lioussse, H. Cachier, and J. Feichter, Construction of a 1° × 1° fossil fuel emission data set for carbonaceous aerosol and implementation and radiative impact in the ECHAM4 model, *J. Geophys. Res.*, **104**, 22,137–22,162, 1999.

- Countess, R. J., Interlaboratory analyses of carbonaceous aerosol samples, *Aerosol Sci. Technol.*, **12**, 114–121, 1990.
- Crutzen, P. J., and M. O. Andreae, Biomass burning in the tropics: Impact on atmospheric chemistry and biogeochemical cycles, *Science*, **250**, 1669–1678, 1990.
- Dickerson, R. R., M. O. Andreae, T. Campos, O. L. Mayol-Bracero, C. Neusuess, and D. G. Streets, Emissions of black carbon and carbon monoxide from south Asia, *J. Geophys. Res.*, **107**, 10.1029/2001JD000501, in press, 2002.
- Dod, R. L., H. Rosen, and T. Novakov, Optico-thermal analysis of the carbonaceous fraction of aerosol particles, *Rep. LBL-8696*, Lawrence Berkeley Lab., Berkeley, Calif., 1979.
- Downing, R. J., R. Ramankutty, J. J. Shah, RAINS-ASIA: An assessment model for acid deposition in Asia, The World Bank, Washington, D.C., 1997.
- Draxler, R. R., and G. D. Hess, Hybrid single-particle Lagrangian integrated trajectories (HY-SPLIT): Version 4, User's guide and model description, NOAA Tech. Memo ERL ARL-224, 1997.
- Eatough, D. J., A. Wadsworth, D. A. Eatough, J. W. Crawford, L. D. Hansen, and E. L. Lewis, A multiple-system, multi-channel diffusion denuder sampler for the determination of fine-particulate organic material in the atmosphere, *Atmos. Environ., Part A*, **27A**, 1213–1219, 1993.
- Ferek, R. J., J. S. Reid, P. Hobbs, D. R. Blake, and C. Lioussé, Emission factors of hydrocarbons, halocarbons, trace gases and particles from biomass burning in Brazil, *J. Geophys. Res.*, **103**, 32,107–32,118, 1998.
- Formenti, P., M. O. Andreae, T. W. Andreae, C. Ichoku, G. Schebeske, A. J. Kettle, W. Maenhaut, J. Cafmeyer, J. Ptasinaky, A. Karnieli, and J. Lelieveld, Physical and chemical characteristics of aerosols over the Negev Desert (Israel) during Summer 1996, *J. Geophys. Res.*, **106**, 4871–4890, 2001.
- Gabriel, R., O. L. Mayol-Bracero, and M. O. Andreae, Chemical characterization of submicron aerosol collected over the Indian Ocean, *J. Geophys. Res.*, **107**, 10.1029/2000JD000034, in press, 2002.
- Gillies, J. A., and A. W. Gertler, Comparison and evaluation of chemically speciated mobile source PM_{2.5} particulate matter profiles, *J. Air Waste Manage. Assoc.*, **50**, 1459–1480, 2000.
- Gillies, J. A., A. W. Gertler, J. C. Sagebiel, and W. A. Dippel, On-road particulate matter (PM_{2.5} and PM₁₀) emissions in the Sepulveda Tunnel, Los Angeles, California, *Environ. Sci. Technol.*, **35**, 1054–1063, 2001.
- Groblicki, P. J., G. T. Wolff, and R. J. Countess, Visibility-reducing species in the Denver "brown cloud," I, Relationships between extinction and chemical composition, *Atmos. Environ.*, **15**, 2473–2484, 1981.
- Gundel, L. A., R. L. Dod, H. Rosen, and T. Novakov, The relationship between optical attenuation and black carbon concentration for ambient and source particles, *Sci. Total Environ.*, **36**, 197–202, 1984.
- Haywood, J. M., and O. Boucher, Estimates of the direct and indirect forcing due to tropospheric aerosols: A review, *Rev. Geophys.*, **38**, 513–543, 2000.
- Hegg, D. A., J. Ferek, and P. V. Hobbs, Light scattering and cloud condensation nucleus activity of sulfate aerosol measured over the north-eastern Atlantic Ocean, *J. Geophys. Res.*, **98**, 14,887–14,894, 1993.
- Hegg, D. A., J. Livingston, P. V. Hobbs, T. Novakov, and P. Russell, Chemical apportionment of aerosol column optical depth off the Mid-Atlantic Coast of the United States, *J. Geophys. Res.*, **102**, 25,293–25,303, 1997.
- Holloway, T., H. Levy II, and P. Kasibhatla, Global distribution of carbon monoxide, *J. Geophys. Res.*, **105**, 12,123–12,147, 2000.
- Holzinger, R., C. Warnecke, A. Hansel, A. Jordan, W. Lindinger, D. Scharffe, G. Schade, and P. J. Crutzen, Biomass burning a source of formaldehyde, acetaldehyde, methanol, acetone, acetonitrile, and hydrogen cyanide, *Geophys. Res. Lett.*, **26**, 1161–1164, 1999.
- Horvath, H., Atmospheric light absorption—A review, *Atmos. Environ., Part A*, **27A**, 293–317, 1993.
- Intergovernmental Panel on Climate Change (IPCC), *Climate Change 1995: The Science of Climate Change*, Cambridge Univ. Press, New York, 1996.
- Jacobson, M. Z., A physically-based treatment of elemental carbon optics: Implications for global direct forcing of aerosols, *Geophys. Res. Lett.*, **27**, 217–220, 2000.
- John, W., S. Hering, G. Reischl, G. Sasaki, and S. Goren, Characteristics of Nuclepore filters with large pore size, II, Filtration properties, *Atmos. Environ.*, **17**, 373–382, 1983.
- Johnson, D. W., S. Osborne, R. Wood, K. Suhre, R. Johnson, S. Businger, P. K. Quinn, A. Wiedensohler, P. H. Durkee, and L. M. Russell, et al., An overview of the Lagrangian experiments undertaken during the North Atlantic regional Aerosol Characterisation Experiment (ACE-2), *Tellus*, **52**, 290–320, 2000.
- Kaneyasu, N., S. Ohta, and N. Murao, Seasonal variation in the chemical composition of atmospheric aerosols and gaseous species in Sapporo, Japan, *Atmos. Environ.*, **29**(13), 1559–1568, 1995.
- Kim, Y. P., K.-C. Moon, J. H. Lee, and N. J. Baik, Concentrations of carbonaceous species in particles at Seoul and Cheju in Korea, *Atmos. Environ.*, **33**, 2751–2758, 1999.
- Kirchstetter, T. W., T. Novakov, R. Morales, and O. Rosario, Differences in the volatility of organic aerosol in unpolluted and polluted continental atmospheres, *J. Geophys. Res.*, **105**, 26,547–26,554, 2000.
- Kirchstetter, T. W., C. E. Corrigan, and T. Novakov, Laboratory and field investigation of the adsorption of gaseous organic compounds onto quartz filters, *Atmos. Environ.*, **35**, 1663–1671, 2001.
- Kleeman, M. J., J. J. Schauer, and G. R. Cass, Size and composition of fine particulate matter emitted from motor vehicles, *Environ. Sci. Technol.*, **34**, 1132–1142, 2000.
- Lavanchy, V. M. H., H. W. Gäggeler, S. Nyeki, and U. Baltensperger, Elemental carbon (EC) and black carbon (BC) measurements with a thermal method and an aethalometer at the high-alpine research station Jungfraujoch, *Atmos. Environ.*, **33**, 2759–2769, 1999.
- Lelieveld, J., P. J. Crutzen, M. O. Andreae, T. Campos, G. R. Cass, R. R. Dickerson, H. Fischer, J. A. de Gouw, A. Hansel, and A. Jefferson, et al., The Indian Ocean Experiment: Widespread air pollution from South and South-East Asia, *Science*, **291**, 1031–1036, 2001.
- Lindberg, J. D., R. E. Douglass, and D. M. Garvey, Carbon and the optical properties of atmospheric dust, *Appl. Opt.*, **32**, 6077–6081, 1993.
- Lioussé, C., H. Cachier, and S. G. Jennings, Optical and thermal measurements of black carbon aerosol content in different environments: Variation of the specific attenuation cross-section, *Atmos. Environ., Part A*, **27A**, 1203–1211, 1993.
- Lobert, J. M., D. H. Scharffe, W. M. Hao, and P. Crutzen, Importance of biomass burning in budgets of nitrogen-containing gases, *Nature*, **346**, 552–554, 1990.
- Lowenthal, D. H., B. Zielinska, J. C. Chow, J. G. Watson, M. Gautam, D. H. Ferguson, G. R. Neuroth, and K. D. Stevens, Characterization of heavy-duty diesel vehicle emissions, *Atmos. Environ.*, **28**, 731–743, 1994.
- Malm, W. C., J. V. Molenaar, R. A. Eldred, and J. F. Sisler, Examining the relationship among atmospheric aerosols and light scattering and extinction in the Grand Canyon area, *J. Geophys. Res.*, **101**, 19,251–19,265, 1996.
- Marland, G., T. A. Boden, R. J. Andres, A. L. Brenkert, and C. Johnston, Global, Regional, and National CO₂ Emissions, in *Trends: A Compendium of Data on Global Change*, Carbon Dioxide Information Analysis Center, Oak Ridge Natl. Lab., U.S. Dep. of Energy, Oak Ridge, Tenn., 1999.
- McDow, S. R., and J. Huntzicker, Vapor adsorption artifact in the sampling of organic aerosol: Face velocity effects, *Atmos. Environ.*, **24**, 2563–2571, 1990.
- Mészáros, E., Á. Molnár, and J. Ogren, Scattering and absorption coefficients vs. chemical composition of fine atmospheric aerosol particles under regional conditions in Hungary, *J. Aerosol Sci.*, **10**, 1171–1178, 1998.
- Murphy, D. M., D. S. Thomson, and T. M. J. Mahoney, In-situ measurements of organics, meteoritic material, mercury, and other elements in aerosols at 5 to 19 kilometers, *Science*, **282**, 1664–1669, 1998.
- National Research Council (NRC), *Aerosol Radiative Forcing and Climate Change*, 161 pp., Natl. Acad., Washington, D.C., 1996.
- Novakov, T., and J. E. Penner, Large contribution of organic aerosols to cloud-condensation nuclei concentrations, *Nature*, **365**, 823–826, 1993.
- Novakov, T., C. E. Corrigan, J. E. Penner, C. C. Chuang, O. Rosario, and O. L. Mayol-Bracero, Organic aerosols in the Caribbean trade winds: A natural source?, *J. Geophys. Res.*, **102**, 21,307–21,313, 1997a.
- Novakov, T., D. A. Hegg, and P. V. Hobbs, Airborne measurements of carbonaceous aerosols on the East Coast of the United States, *J. Geophys. Res.*, **102**, 30,023–30,030, 1997b.
- Novakov, T., T. S. Bates, and P. K. Quinn, Shipboard measurements of concentrations and properties of carbonaceous aerosols during ACE-2, *Tellus, Ser. B*, **52**, 228–237, 2000a.
- Novakov, T., M. O. Andreae, R. Gabriel, T. W. Kirchstetter, O. L. Mayol-Bracero, and V. Ramanathan, Origin of carbonaceous aerosols over the Tropical Indian Ocean: Biomass burning or fossil fuels?, *Geophys. Res. Lett.*, **27**, 4061–4064, 2000b.
- Olivier, J. G. J., A. F. Bouwman, C. W. M. van der Maas, and J. J. M. Berdowski, Emission data for global atmospheric research, *Environ. Monit. Assess.*, **31**, 93–116, 1994.
- Penner, J. E., C. C. Chuang, and K. Grant, Climate forcing by carbonaceous and sulfate aerosols, *Clim. Dyn.*, **14**, 839–851, 1998.
- Podgorny, I. A., W. Connant, V. Ramanathan, and S. K. Satheesh, Aerosol modulation of Atmospheric and surface solar heating, *Tellus*, **52**, 947–958, 2000.
- Quinn, P. K., T. S. Bates, D. J. Coffman, T. L. Miller, J. E. Johnson, D. S. Covert, J.-P. Putaud, C. Neusüß, and T. Novakov, A comparison of

- aerosol chemical and optical properties from the 1st and 2nd Aerosol Characterization Experiments, *Tellus, Ser. B*, 52, 239–257, 2000.
- Ramanathan, V., et al., Indian Ocean Experiment: An integrated analysis of the climate forcing and effects of the great Indo-Asian haze, *J. Geophys. Res.*, 106, 28,371–28,398, 2001.
- Rasch, P. J., W. D. Collins, and B. E. Eaton, Understanding the Indian Ocean Experiment INDOEX aerosol distributions with an aerosol assimilation, *J. Geophys. Res.*, 106, 7337–7355, 2001.
- Reddy, M. S., and C. Venkataraman, Atmospheric optical and radiative effects of anthropogenic aerosol constituents from India, *Atmos. Environ.*, 34, 4511–4523, 2000.
- Reddy, M. S., and C. Venkataraman, Inventory of aerosol and sulphur dioxide emissions from India, I, Fossil fuel combustion, *Atmos. Environ.*, 36, 677–697, 2002a.
- Reddy, M. S., and C. Venkataraman, Inventory of aerosol and sulphur dioxide emissions from India, II, Biomass combustion, *Atmos. Environ.*, 36, 697–710, 2002b.
- Reiner, T., D. Sprung, C. Jost, R. Gabriel, O. L. Mayol-Bracero, M. O. Andreae, T. L. Campos, and R. E. Shetter, Chemical characterization of pollution layers over the tropical Indian Ocean: Signatures of emissions from biomass and fossil fuel burning, *J. Geophys. Res.*, 106, 28,497–28,510, 2001.
- Rivera-Carpio, C. A., C. E. Corrigan, T. Novakov, J. E. Penner, C. F. Rogers, and J. C. Chow, Derivation of contributions of sulfate and carbonaceous aerosols to cloud condensation nuclei from mass size distributions, *J. Geophys. Res.*, 101, 19,483–19,493, 1996.
- Rogge, W. F., M. A. Mazurek, L. M. Hildemann, G. Cass, and B. R. T. Simoneit, Quantification of urban organic aerosols at a molecular level: Identification, abundance and seasonal variation, *Atmos. Environ.*, 27, 1309–1330, 1993.
- Rosen, H., A. D. A. Hansen, L. Gundel, and T. Novakov, Identification of the optically absorbing component in urban aerosols, *Appl. Opt.*, 17, 3859–3861, 1978.
- Ruellan, S., H. Cachier, A. Gaudichet, P. Masclet, and J. P. Lacaux, Airborne aerosols over central Africa during Experiment for Regional Sources and Sinks of Oxidants (EXPRESSO), *J. Geophys. Res.*, 104, 30,673–30,690, 1999.
- Salmon L. G., L. M. Hildemann, M. Mazurek, C. Christoforou, N. A. Frei, P. A. Solomon, J. Schauer, L. Hughes, and R. Johnson, Procedures Manual, Environ. Qual. Lab., Calif. Inst. of Technol., Pasadena, Calif., Aug. 1998.
- Satheesh, S. K., V. Ramanathan, X. Li-Jones, J. M. Lobert, I. A. Podgorny, J. M. Prospero, B. N. Holben, and N. G. Loeb, A model for the natural and anthropogenic aerosols over the tropical Indian Ocean derived from Indian Ocean Experiment data, *J. Geophys. Res.*, 104, 27,421–27,440, 1999.
- Satheesh, S. K., and V. Ramanathan, Large differences in tropical aerosol forcing at the top of the atmosphere and Earth's surface, *Nature*, 405, 60–63, 2000.
- Schmid, H., L. Laskus, H. J. Abraham, U. Baltensperger, V. Lavanchy, M. Bizjak, P. Burba, H. Cachier, D. Crow, and J. Chow, et al., Results of the carbon conference international aerosol carbon round robin test stage I, *Atmos. Environ.*, 35, 2111–2121, 2001.
- Shah, J. J., J. G. Watson Jr., J. A. Cooper, and J. J. Huntzicker, Aerosol chemical composition and light scattering in Portland, Oregon: The role of carbon, *Atmos. Environ.*, 18, 235–240, 1984.
- Shah, J. J., and J. A. Rau, Carbonaceous species methods comparison study: Interlaboratory round robin interpretation of results, final report, contract A832-154, Calif. Air Resour. Board, Sacramento, Calif., 1990.
- Sheridan, P., A. Jefferson, and J. Ogren, Spatial variability of aerosol radiative properties over the Indian Ocean during INDOEX, *J. Geophys. Res.*, 107, 10.1029/2000JD000166, in press, 2002.
- Spiro, P. A., D. J. Jacob, and J. A. Logan, Global inventory of sulfur emissions with $1^\circ \times 1^\circ$ resolution, *J. Geophys. Res.*, 97, 6023–6036, 1992.
- Streets, D. G., and S. Waldhoff, Biofuel use in Asia and acidifying emissions, *Energy*, 23, 1029–1042, 1998.
- Streets, D. G., S. K. Guttikunda, and G. R. Carmichael, The growing contribution of sulfur emissions from ships in Asian waters, 1988–1995, *Atmos. Environ.*, 34, 4425–4439, 2000.
- Streets, D. G., S. Gupta, S. T. Waldhoff, M. Q. Wang, T. C. Bond, and Y. Bo, Black carbon emissions in China, *Atmos. Environ.*, 35, 4281–4296, 2001.
- Turpin B. J., and H.-J. Lim, Species contributions to PM_{2.5} mass concentrations: Revisiting common assumptions for estimating organic mass, *Aero-sol Sci. Technol.*, 35, 602–610, 2001.
- Turpin, B. J., J. J. Huntzicker, and S. V. Hering, Investigation of the organic aerosol sampling artifacts in the Los Angeles basin, *Atmos. Environ.*, 28, 3061–3071, 1994.
- U.S. Environmental Protection Agency, Supplement B to compilation of air pollutant emission factors, Volume I, Stationary point and area sources, Tech. Rep., Off. of Air Qual. Plann. and Stand., Research Triangle Park, N. C., 1996.
- Venkataraman, C., B. Chandramouli, and A. Patwardhan, Anthropogenic sulphate aerosol from India: estimates of burden and direct radiative forcing, *Atmos. Environ.*, 33, 3225–3235, 1999.
- Verver, G. H. L., D. R. Sikka, J. M. Lobert, G. Stossmeister, and M. Zachariasse, Overview of the meteorological conditions and atmospheric transport processes during INDOEX 1999, *J. Geophys. Res.*, 107, 10.1029/2001JD900203, in press, 2002.
- Waggoner, A. P., R. E. Weiss, N. C. Ahlquist, D. S. Covert, S. Will, and R. J. Charlson, Optical characteristics of atmospheric aerosols, *Atmos. Environ.*, 15, 1891–1909, 1981.
- White, W. H., Contribution to light extinction, in *Acid Deposition, State of Science and Technology, NAPAP Rep. 24, 85-102*, Natl. Acid Precip. Assess. Program, Washington, D. C., 1990.
- Zappoli, S., A. Andracchio, S. Fuzzi, M. C. Facchini, A. Gelencsér, H. Kiss, Z. Krivácsy, A. Molnár, E. Mészáros, and H.-C. Hansson, et al., Inorganic, organic and macromolecular components of fine aerosol in different areas of Europe in relation to their water solubility, *Atmos. Environ.*, 33, 2733–2743, 1999.

O. L. Mayol-Bracero, R. Gabriel, and M. O. Andreae, Biogeochemistry Department, Max Planck Institute for Chemistry, P.O. Box 3060, 55020 Mainz, Germany. (omayol@mpch-mainz.mpg.de)

T. W. Kirchstetter and T. Novakov, Atmospheric Aerosol Research, Lawrence Berkeley National Laboratory, Berkeley, CA 94720, USA. (tnovakov@lbl.gov)

J. Ogren and P. Sheridan, Climate Monitoring and Diagnostics Laboratory, NOAA, Boulder, CO, USA. (John.A.Ogren@noaa.gov)

D. G. Streets, Decision and Information Sciences Division, Argonne National Laboratory, Argonne, IL 60439, USA. (dstreets@anl.gov)